RSC Advances

REVIEW

View Article Online
View Journal | View Issue

Cite this: *RSC Adv.*, 2024, **14**, 1284

Recent progress in graphene and its derived hybrid materials for high-performance supercapacitor electrode applications

Prasanta Kumar Sahoo, *[ab] Niraj Kumar,[cg] Anirudha Jena, [d] Sujata Mishra, [e] Chuan-Pei Lee,[f] Seul-Yi Lee*[g] and Soo-Jin Park*[g]

Received 10th October 2023
Accepted 6th December 2023

DOI: 10.1039/d3ra06904d

rsc.li/rsc-advances

Graphene, the most fascinating 2D form of carbon with closely packed carbon atoms arranged in a layer, needs more attention in various fields. For its unique electrical, mechanical, and chemical properties with a large surface area, graphene has been in the limelight since its first report. Graphene has extraordinary properties, making it the most promising electrode component for applications in supercapacitors. However, the persistent re-stacking of carbon layers in graphene, caused by firm interlayer van der Waals attractions, significantly impairs the performance of supercapacitors. As a result, many strategies have been used to get around the aforementioned problems. The utilization of graphene-based nanomaterials has been implemented to surmount the aforementioned constraints and considerably enhance the performance of supercapacitors. This review highlights recent progress in graphene-based nanomaterials with metal oxide, sulfides, phosphides, nitrides, carbides, and conducting polymers, focusing on their synthetic approach, configurations, and electrochemical properties for supercapacitors. It discusses new possibilities that could increase the performance of next-generation supercapacitors.

1. Introduction

As a result of the current energy crisis, the need for energy storage systems with novel energy storage capabilities is gradually rising. To supply the energy required for electric automobiles, other vehicles, and other supplies, devices for energy storage applications, such as batteries, supercapacitors (SCs), and water splitting, are available. Because of their high specific power, long life, quick discharge–charge rates, environmental friendliness, memory backup equipment, and low maintenance cost, supercapacitors have become very popular in recent years. They are now widely used as highly efficient clean energy storage devices.[1–4] In general, SCs can be divided into three groups according to the method used to transmit the charge. The electrochemical double-layer capacitors (EDLCs) store energy electrostatically in two of the closest layers to the electrode surface, the pseudocapacitors store energy through a redox process, and the hybrid capacitors, created by combining EDLCs and pseudocapacitors, store energy through both faradaic and non-faradaic pathways. The enormous specific power, prolonged lifespan, and hybrid mode usage of SCs account for their exceptional performance.[5,6] However, the SCs' lower energy density prevents them from being used in high-energy applications.[7] The packaging of the cell components of SCs, including electrodes, electrolytes, separators, and current collectors, may impact electrochemical performance. The performance of a supercapacitor can also be affected by the process employed to synthesize the active materials and the constituent precursors. Therefore, additional study and analysis are needed on the cell management system, device design, and internal components to suit the needs of the present and the future.[8,9] Both metallic and nonmetallic materials can be precursors for electrode synthesis, but they should have modest electrical conductivity. It is possible to modify the morphology of these materials to advance the execution of supercapacitors.[10] It is possible to combine several carbon-based materials like CNTs, graphene, *etc.* to improve the performance of the metallic and non-metallic-based supercapacitors. Moreover, the self-restacking of graphene oxide causes a decrease in capacitance and lowers the kinetics of ion transport. This is a major

[a]*Department of Mechanical Engineering, Siksha 'O' Anusandhan, Deemed to be University, Bhubneswar, 751030, India. E-mail: prasantakumarsahoo@soa.ac.in; Fax: +91-67-42351880; Tel: +91-67-42350181*

[b]*Environmental Hydrology Division, National Institute of Hydrology, Jalvigyan Bhawan, Roorkee 247667, India*

[c]*Sustainable Energy Laboratory, Department of Metallurgical and Materials Engineering, Defence Institute of Advanced Technology (DIAT), Pune, Maharashtra 411025, India*

[d]*School of Applied Sciences, Kalinga Institute of Industrial Technology, Deemed to be University, Bhubaneswar 751024, Odisha, India*

[e]*Department of Chemistry, Institute of Technical Education and Research (FET), Siksha 'O' Anusandhan Deemed to Be University, Khandagiri Square, Bhubaneswar, 751030, Odisha, India*

[f]*Department of Applied Physics and Chemistry, University of Taipei, Taipei 10048, Taiwan*

[g]*Department of Chemistry, Inha University, Incheon 22212, Republic of Korea. E-mail: leesy1019@inha.ac.kr; sjpark@inha.ac.kr*

drawback to fabricating a supercapacitor that can be employed for high-performance applications. The optimal purpose of graphene-metal composites is increasingly essential to enable them to perform at their full potential. This includes a greater energy density, a higher power density, and long cyclic retention. The distribution of pore size and pore volume is important as well. The properties of the electrode material are determined by the pore size distribution and accessible surface area of the electrode available for ion adsorption. In addition, choosing the proper electrolytes can boost the operating voltage, which is regulated by electrolyte stability. In contrast to an aqueous electrolyte, organic and hybrid electrolytes provide a large operating potential window. By introducing metal derivatives to graphene, it is possible to enhance the active surface area of the material, improve ion transfer channels, and increase its chemical, thermal, and mechanical stability.[11] A two-dimensional grid of carbon atoms with sp^2 hybridization is known as graphene. The thinnest two-dimensional nanomaterial, graphene, has great mechanical properties, a large surface area, chemical stability, higher electron mobility, and superior electrical conductivity, making it an excellent choice for an electrode material for a supercapacitor. Due to its strong contact, 2-D graphene is quickly restacked when electrodes are operating, which lowers the active surface area that is accessible to it as well as the rate of ion diffusion, both of which are responsible for lowering specific capacitance and the rate of charge/discharge rate. The constraints of ion diffusion and electron transfer resistance become increasingly relevant as the amount of active material in supercapacitors increases. As a result, the device's overpotential is greatly increased while its capacitance decreases during charging.

However, the electrode materials using heterostructured materials feature conductive layers and porous networks, enabling the ions and charges to move easily across a huge electrode area and thereby providing an easy way to store energy.[12–15] Graphene-metal derivatives can avoid stacking effects caused by two-dimensional nanosheets, which makes them ideal for supercapacitors. Consequently, it is very important that technologies for easily preparing these heterostructure materials be developed to enable them to be used as supercapacitors. In particular, the heterostructure of graphene enables charge and ion transfer to the active material, allowing it to fully expend its energy storage capacity and generate higher energy and power density. Because of their remarkable qualities, a variety of metal oxides, sulphides, carbides, nitrides, phosphides, and conducting polymers (CPs) have been investigated as electrodes for applications in SCs.[16–21]

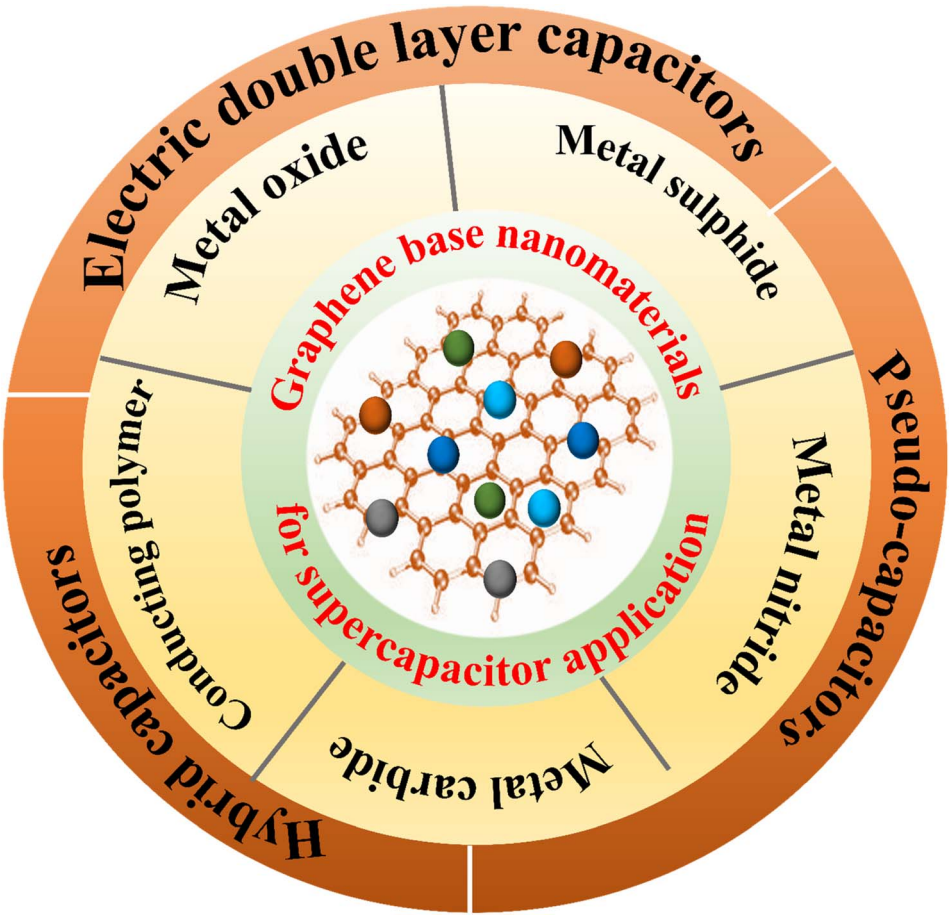

Scheme 1 Graphical illustration of the content of this review.

Recently, composites made of graphene have been researched to achieve exceptional electrochemical performance.[22–26] Due to its poor EDLC-type nature, the use of graphene as electrodes in supercapacitors is constrained by low capacitance and low energy density. To address these issues, composite materials based on graphene are created for supercapacitor applications. This review summarises recent advancements in graphene-based electrode materials in association with metal oxide, sulfides, phosphides, nitrides, carbides, and conducting polymers, from the synthetic approach, results of morphology, structure, and composition of the electrochemical attributes for supercapacitor application. Finally, a summary is provided of the perspective for the present issues and potential future developments related to graphene-based nanomaterials used as supercapacitor electrode materials. A schematic representation of the review's contents is presented in Scheme 1.

2. Graphene-based nanomaterials as supercapacitor applications

Graphene-based materials, including graphene oxide and reduced graphene oxide, possess properties that distinguish them from other materials and make them ideal for use in various technologies. Their high theoretical specific surface areas provide extensive contact points for interactions, resulting in remarkable thermochemical stability and robust mechanical properties. These characteristics make them valuable components for applications such as supercapacitors, lithium–sulfur batteries, and CO_2 adsorbents. Activated carbon, derived from carbon-rich sources through chemical treatments, also possesses a porous nature and a large surface area, making it efficient for the adsorption of gases and liquids. The combination of graphene-based materials and activated carbon in composites leverages their respective strengths, such as in graphene-based activated carbon composites, which enhance lithium–sulfur battery performance. Table 1 compares graphene-based materials to other high-surface-area materials in the context of supercapacitor applications.[27–31]

Hierarchically porous graphene-based carbons derived from biomass sources offer three-dimensional interconnected pores and thin graphitic carbon walls, resulting in supercapacitors with exceptional energy and power densities. The high surface areas of both graphene-based materials and activated carbon uniquely contribute to various fields, such as energy storage, CO_2 capture, and water purification. While graphene-based materials provide stability and mechanical strength, activated carbon exhibits a specific surface area and adsorption capabilities. The utilization of these materials in various applications is promising for advancements in energy storage. Graphene-based materials demonstrate better performance than activated carbon in several aspects.[32,33] Their specific surface areas were significantly higher, allowing for more efficient charge storage and adsorption of gases and liquids. The lightweight nature of graphene, resulting from its single-layer structure, makes it an ideal choice for applications in which weight is a critical factor. The eco-friendliness of graphene, derived from its graphite composition, enhances its environmental profile for energy storage applications. With a theoretical upper limit of 550 F g^{-1}, graphene-based supercapacitors outperform existing technologies and offer improved energy-storage performance and longer lifespans.[34] The mechanical strength and elasticity of graphene contribute to its durability and reliability for various applications. The adjustable three-dimensional networks formed by graphene-based materials provide additional opportunities for adsorption and interaction with gases and liquids. The high chemical and thermal stability of graphene makes it suitable for use in harsh environments and high-temperature conditions.

The energy density of graphene for supercapacitor applications is due to its EDLC-type storage mechanism, which is restricted to the surface. However, pseudocapacitive materials have a higher energy density because of a reversible reaction between two electrodes, and electrolytes help to store more charge. By adding pseudocapacitive materials, the energy density of EDLC-type graphene for supercapacitor applications can be effectively increased. Recently, pseudocapacitive materials such as metal oxides,[35] sulfides,[36] phosphides,[37] carbides,[38] nitrides,[39] and conducting polymers[40] are gaining much attention as electrode materials for supercapacitor electrode materials as they are cheaper, possesses high theoretical capacitance, have a faster cycle rate, and are eco-friendly. However, their poor electronic, as well as ionic conductance limits the power density and reversibility. Therefore, a hybrid of graphene-based composite materials wherein metal oxides, sulfides, phosphides, nitrides, carbides, and conducting polymers are jointly used with graphene as the electrode for supercapacitor applications.

2.1 Graphene-metal oxide-based nanomaterials

Metal oxides are promising for their high theoretical capacitance, cost-effectiveness, eco-friendly nature, and abundance.[35] Because of reversible faradaic responses at the electrode–electrolyte interface, metal oxides exhibit large specific capacitance. Consequently, the combination of metal oxides and graphene produced graphene-metal oxide-based nanomaterials that effectively enhance supercapacitor performance to a significant degree. In a controlled pH synthesis process, Hassan *et al.* prepared the RuO_2/rGO in a single pot using a faster and more environmentally friendly method. No additional reducing agent or calcination step was necessary for the production of crystalline RuO_2 nanoparticles using this method.[41] The RuO_2/rGO prepared at pH 8 provided a specific capacitance of 270 F g^{-1} at 5 mV s^{-1}. The specific capacitance of RuO_2/rGO increased over the first 2600 cycles to reach 108% of the initial specific capacitance. After cycling for 5000 cycles consecutively, the specific capacitance retention was 92.5%. After 5000 cycles, the RuO_2/rGO electrode was left in the electrolyte solution for an entire night, and then GCD was recorded at 24 A g^{-1} for another 100 cycles. It is noticed that the electrode's performance was increased to 146% of the initial specific capacitance after 5 cycles (total of 5005 cycles) and the increase in performance was stable up to 100 cycles (total of 5100 cycles). The RuO_2-based

Table 1 Comparison of graphene-based material with other high-surface-area materials

Property	Graphene-based materials	Activated carbon	Conductive polymers	Metal oxides	Ref.
Surface area	High surface area due to a single layer of carbon atoms arranged in a hexagonal lattice	High surface area achieved through activation processes	Variable, typically lower than graphene or activated carbon	Highly dependent on the specific metal oxide, but often lower than graphene	27
Conductivity	Excellent	Moderate to high	Variable, can be tuned, but generally lower than graphene	Moderate to low	28
Cycling stability	Good, minimal degradation over many charge/discharge cycles	Good, suitable for long-term use	May suffer from degradation over extended cycling	Varies depending on the metal oxide. Some may experience degradation	29
Electrochemical performance	High, quick charge/discharge rates	Moderate, generally slower charge/discharge rates than graphene	Depends on the specific polymer, can be moderate to high	Varies widely based on the metal oxide	30
Cost	Generally higher cost due to the production process	Cost-effective, especially in comparison to graphene	Cost-effective, especially compared to graphene	Cost varies depending on the specific metal oxide. Some can be cost-effective, while others may be more expensive	31
Synthesis method	Multiple methods, including chemical vapor deposition (CVD), liquid-phase exfoliation, and chemical reduction of graphene oxide	Typically produced through the activation of carbon precursors, such as coconut shells or coal	Various methods, including chemical synthesis and electrochemical methods	Synthesis methods vary based on the specific metal oxide	32
Applications	Supercapacitors, batteries, electronic devices	Supercapacitors, water purification, air filtration	Supercapacitors, flexible electronics	Supercapacitors, batteries, catalysis	33

rGO nanoparticles have a greater power density of 76.4 kW kg^{-1} and an increased energy density of 15 W h kg^{-1}.

Reduced graphene oxide (rGO) and manganese oxide (MnO_x) nanocomposites were created utilizing a single *in situ* chemical technique, according to Singu *et al*. The generated nanocomposite material had a specific capacitance value of 398.8 F g^{-1} at a sweep rate of 5 mV s^{-1}. It was shown that rGO/MnO_x nanocomposite with high exfoliation has a higher electrochemical capacitance value than rGO/Mn_3O_4 composite. With a specific capacitance retention of 78% of the initial value after 5000 GCD cycles at 2 A g^{-1} current density, the rGO/MnO_x composites exhibit greater cyclic stability.[42] By electrochemically covering graphene with manganese oxide, Kumar *et al.* were able to produce graphene foam from polyurethane foam, revealing hierarchical porosity architectures.[43] The produced composite has a specific capacitance value of 672 F g^{-1} for 0.5 mg cm^{-2} manganese oxide loading, a good rate of retention over 1–20 A g^{-1}, a longer life cycle (only 2% capacity loss after 10 000 GCD cycles), and a good rate of retention over 1–20 A g^{-1}. Gryglewicz *et al.* developed a ternary composite of polypyrrole/iron oxide/rGO, iron oxide/rGO, and oxidative polymerization on iron oxide/rGO using a two-step hydrothermal procedure. In comparison to the iron oxide/rGO binary composite, the generated composite electrode has a specific capacitance value of 140 F g^{-1} at 0.2 A g^{-1}, which is 70% higher, showing a greater contribution of pseudocapacitive polypyrrole to overall capacitance.[44] The ternary composite has an exceptional rate of capacitance retention of 93 percent over 5000 cycles at 1 A g^{-1}. Microwaves are used to quickly mix carbon dots with reduced graphene oxide to create cobalt oxide nanocomposite electrodes, as described by Yetiman *et al.* in Fig. 1a.[45] Clear redox peaks in Fig. 1b verify the faradaic behavior, and there is a linear connection between anodic and cathodic peak current density and scan rate. Fig. 1c, confirms surface redox reactions can be delivered with a maximum specific capacitance of 936 F g^{-1} by a carbon-dot-containing electrode at a 0.5 A g^{-1} current density. The ability of the electrodes to maintain a stable capacitance throughout 10 000 cycles is relatively high, as they retain 93% and 87% of the initial capacitance (Fig. 1d). Research has demonstrated that carbon dots and reduced graphene oxide-doped transition metal oxide nanoparticles can be used as promising electrodes for supercapacitors. Salarizadeh *et al.* developed cerium oxide (CeO_2) by hydrothermal method from a thin layer of cerium oxide (CeO_2) and reduced graphene oxide (rGO) nanosheets.[46] CeO_2/rGO has a high specific capacitance of 581 F g^{-1} when exposed to 2 M KOH solutions with a scan rate of 10 mV s^{-1} and 91% cyclic retention after 5000 cycle tests. They observed that CeO_2 nanoparticles coated with rGO could facilitate the migration of electrolytes and provide enormous active sites for faradic operation. Additionally, rGO nanosheets improve a porous composite's conductance and stability for electrochemical activity.

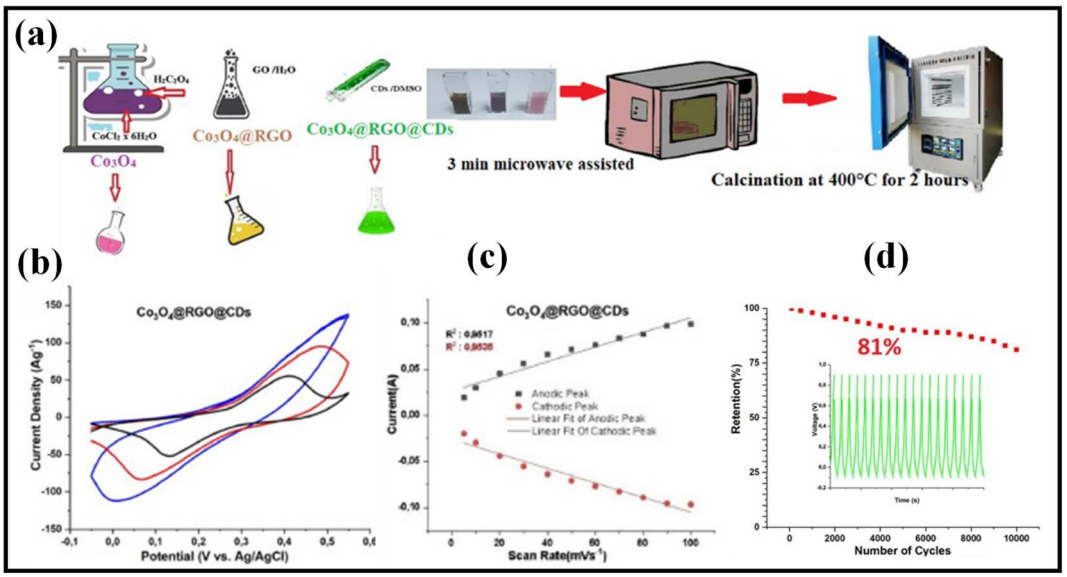

Fig. 1 (a) Synthesis step scheme of Co_3O_4 and Co_3O_4@rGO@CDs using Co_3O_4@rGO and Co_3O_4@rGO@CDs, (b) CV curves, (c) anodic/cathodic current peaks at various scan rates, and (d) capacitance stability and cycle stability of the symmetric supercapacitor current density of 2.5 A g^{-1} for 10 000 cycles.[45] Copyright 2022. Reproduced with permission from Elsevier.

For the development of the Fe_3O_4/rGO nanocomposite, Low *et al.* established an easy hydrothermal procedure (Fig. 2a). Easy charge transportation in the nanorods improves the electrode's performance and increases the nanocomposite's specific capacitance.[47] Depending on the composite's composition, Fe_2O_3 nanorods/rGO, Fe_2O_3 nanoparticles/rGO, and Fe_2O_3 collected nanorods/rGO offer specific capacitances of 504, 138, and 193 F g^{-1}, respectively. Kumar *et al.* created the rGO@Co_3O_4/CoO composite using a straightforward one-step microwave irradiation procedure. Co_3O_4/CoO nanoparticles

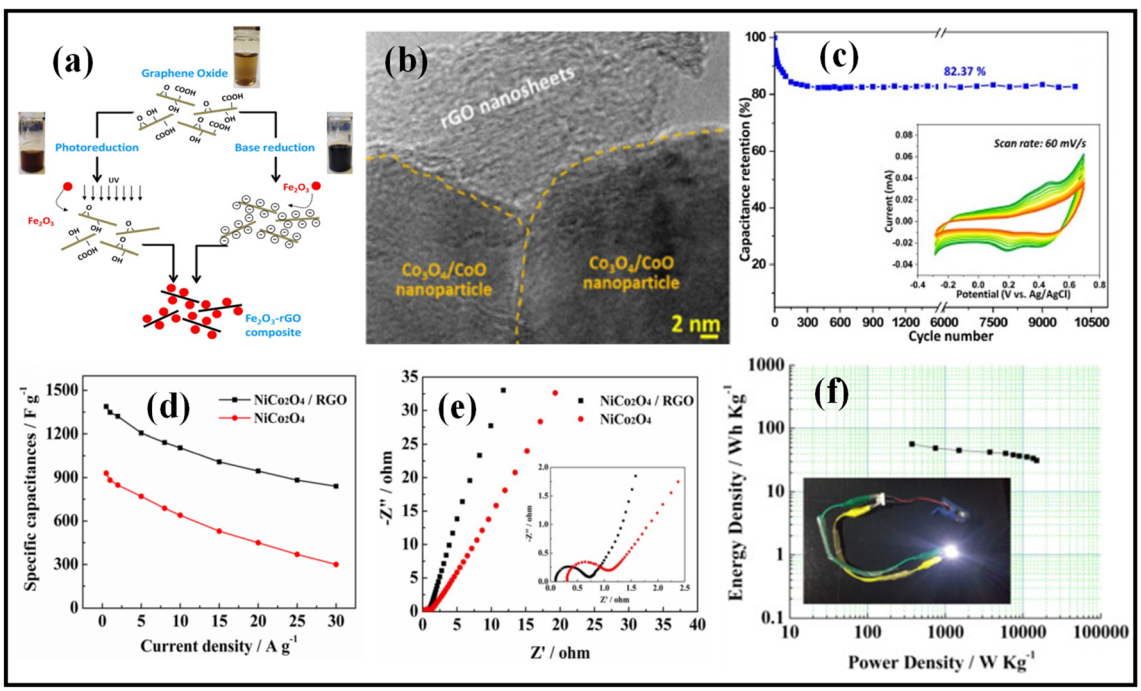

Fig. 2 (a) Schematic of synthesis of Fe_3O_4/rGO nanocomposite through base reduction and photoreduction methods.[47] Copyright 2014. Reproduced with permission from Elsevier, (b) HR-TEM image of rGO@Co_3O_4/CoO composite.[48] Copyright 2021. Reproduced with permission from Elsevier, (c) cyclic stability study of rGO@Co_3O_4/CoO composite at a scan rate of 60 mV s^{-1}, (d and e) specific capacitances *vs.* current density and Nyquist plots of pure $NiCo_2O_4$ and $NiCo_2O_4$/rGO composite.[50] Copyright 2017. Reproduced with permission from Elsevier, (f) Ragone plot of the fabricated $NiCo_2O_4$/rGO//AC asymmetric supercapacitor (inset: LED light gown by series-connected $NiCo_2O_4$/rGO//AC asymmetric supercapacitor).

are embedded with rGO nanosheets, as seen in the HRTEM image in Fig. 2b, and 0.28 nm lattice fringes reveal that the Co_3O_4 is in the (220) plane. At a scan rate of 5 mV s^{-1}, the as-prepared rGO@Co_3O_4/CoO composite materials exhibit a specific capacitance value of 276.1 F g^{-1}. The capacitor's cyclic stability is maintained at 82.37 percent even after 10 000 cycles, as shown in Fig. 2c. The rGO@Co_3O_4/CoO hybrid may prove to be a very useful electrode material in supercapacitor applications, according to this.[48] A cobalt oxide nanocube intercalated reduced graphene oxide electrode was created by Ramesh *et al.* using a simple hydrothermal technique.[49] The HRTEM image in Fig. 2b shows Co_3O_4/CoO nanoparticles are embedded with rGO nanosheets, and 0.28 nm lattice fringes confirm the (220) plane of Co_3O_4. The as-prepared rGO@Co_3O_4/CoO composite materials have a specific capacitance value of 276.1 F g^{-1} at a scan rate of 5 mV s^{-1}. Fig. 2c shows that the capacitor cyclic stability is sustained at 82.37 percent even after 10 000 cycles. This indicates the potential of the rGO@Co_3O_4/CoO hybrid as a high-performance electrode material for supercapacitor applications.[48] Ramesh *et al.* used a facile hydrothermal process to prepare a cobalt oxide nanocube intercalated with a reduced graphene oxide electrode.[49] With an average size of 45 nm, cubical Co_3O_4 particles were used to embellish an rGO matrix. The constructed Co_3O_4/rGO electrode has a specific capacitance value of 278 F g^{-1} at a current density of 200 mA g^{-1} and a potential window of 0–1.0 V. Bimetallic $NiCo_2O_4$/rGO nanocomposite was created in an original layer-by-layer fashion by Li *et al.* using freeze-drying and annealing processes. The bimetallic $NiCo_2O_4$/rGO composite nanomaterial has a large surface area and good electronic conductivity because it has more electroactive sites.[50] More so than pure $NiCo_2O_4$, it has a high specific capacity of 1388 F g^{-1} at 0.5 A g^{-1} and exceptional rate performance of 840 F g^{-1} at a current density of 30 A g^{-1} with good cyclic retention of 90.2 percent after 20 000 cycles (Fig. 2d). The decreased R_{ct} value of the $NiCo_2O_4$/rGO nanocomposite compared to $NiCo_2O_4$ implies a speedier ion diffusion process and favorable charge-transfer kinetics, as illustrated in Fig. 2e. The $NiCo_2O_4$/rGO//AC asymmetric supercapacitor's Ragone plot in Fig. 2f demonstrates that it outperforms $NiCo_2O_4$ with an energy density of 57 W h kg^{-1} at a power density of 375 W kg^{-1}. An LED was illuminated to evaluate the $NiCo_2O_4$/rGO//AC asymmetric supercapacitor's practical applicability (see inset in Fig. 2f). According to Wang *et al.*, the $MnCo_2O_4$/3D-graphene composite electrode was created in a straightforward two-step procedure. In the morphology and microstructure of the generated samples, as well as at low and high magnification, the $MnCo_2O_4$/3DG electrode composites were found to have a cubic structure with 100 to 200 nm length and stacked together.[51]

The composite electrode showed outstanding cycling stability across 5000 charging–discharging cycles at 10 A g^{-1} current density, maintaining 97.40 percent of specific capacitance, and a specific capacitance of 503 F g^{-1} at a 1 A g^{-1} current density. A simple solvothermal method was used by Low *et al.* to create an electrode that contained nano-sized MnV_2O_6 and graphene nanosheets (G-MVO).[52] To explore the synergistic effect of these two materials and their effect on the addition to the energy storage capabilities of the nanocomposites, the weight ratios of the graphene: MnV_2O_6 and graphene: Mn_2O_6 nanocomposites were optimized. The synthesized version of graphene/MnV_2O_6 nanocomposites, G-8MVO nanocomposite, has once again been identified as a useful electrode material for supercapacitor applications.

2.2 Graphene-metal sulphides-based nanomaterials

The metal sulfide class of materials with superior redox activity and tuned conduction properties are becoming exceptional electrode materials in the field of energy storage applications.[28] Furthermore, for their unique structural variety and charge-retaining capability, they show higher energy density than their competitors. Therefore, combining metal sulfides with graphene to make graphene-metal sulfides-based nanomaterials can significantly improve the supercapacitor performance to a large amount. To create the composite between nickel sulphide and Ni foam coated with graphene oxide thin films, Razaq *et al.* devised a simple hydrothermal technique.[53] The addition of a thin coating of GO greatly increases the active specific surface area and conductivity of the GO-nickel sulfide nanoplates (GO-NSNPs) composite. In a 3-electrode device, a specific capacitance of 1745.5 F g^{-1} and a specific energy of 87.27 W h kg^{-1} were obtained at a current density of 5 mA cm^{-2}. Graphene oxide-nickel sulphide nanoplates demonstrated the highest specific energy of 15.72 W h kg^{-1} and specific power of 848.5 W kg^{-1} using the symmetric electrodes system. The tin sulfide/graphene nanocomposite was made utilizing a straightforward hydrothermal technique by Balu *et al.* At a scan rate of 5 mV s^{-1} in 2 M KOH and a long discharge time rate, the as-prepared nanocomposite electrode demonstrated good specific capacitance values of 1398.93 F g^{-1} and good cyclic stability performance of 94.37% over 1000 cycles.[54] Tin sulphide and tin sulfide/graphene nanocomposite were evaluated using EIS in the frequency range of 100 kHz to 0.01 Hz.[54] Reduced graphene oxide and copper sulphide nanosheets were combined to create the rGO-CuS nanocomposite, which was created by Lokhande *et al*. A specific capacitance of 1201 F g^{-1} at 5 mV s^{-1} is produced by the hybrid composite electrode (rGO-CuS) in 1 M $LiClO_4$. A hybrid flexible symmetric solid-state supercapacitor (FSS-SSC) made up of SS/rGO-CuS/polyvinyl alcohol (PVA)-$LiClO_4$/CuS-rGO/SS with PVA-$LiClO_4$ gel electrolyte, has a specific energy of 44 W h kg^{-1}, at 165°, the device retains 90 percent of its specific capacitance, and it holds 87 percent of its intial specific capacitance after 6000 cycles.[55] Layered hybrid structures have a long electrochemical life and largely use diffusion to store charge. For use in electrochemical supercapacitors, Zhang *et al.* created a Ni_3S_2/3D graphene/nickel foam composite electrode using a simple chemical vapour deposition technique. A huge specific surface area and excellent Ni_3S_2 hexagonal woodite phase, which promotes electron transport between Ni_3S_2 and 3D graphene/nickel foam, are suggested to be the reasons why pure Ni_3S_2 exhibits good capacitive performance. When compared to Ni_3S_2/NF, the Ni_3S_2/Ni_3G/NF electrode showed a specific capacitance value of 2585 F g^{-1} at a current density of 1 A g^{-1} and a retention rate of 88.9% after 5000 cycles, which also shows that the impedance that

causes ions to diffuse from electrode to electrolyte is relatively small.[56] Muralidharan *et al.* used a straightforward, PEG-assisted, one-step hydrothermal procedure to create the graphene encapsulated with NiS/Ni_3S_4 nanostructure. It was demonstrated that the high-specific capacitance composite (NSG) had an amazing long-term retention of 88 percent cyclic stability after 5000 cycles with a coulombic efficiency of 95%, and a current density of 5 A g^{-1}, which is more prominent than that of pristine polyethylene glycol (574 C g^{-1}). With a current density of 2 A g^{-1} and a power density of 375 W kg^{-1}, the asymmetric device has the highest energy density, at 86.3 W h kg^{-1}. Due to its increased specific surface area, the synergistic effect of both components, and the ease of conducting channels, graphene-capsulated nickel sulphide has significant specific energy.[57] Zhang *et al.* used a straightforward solvothermal technique to demonstrate a composite of $NiCo_2S_4$@rGO. At a current density of 1 A g^{-1}, the synthetic $NiCo_2S_4$@rGO composite material has a specific capacity of 2418 F g^{-1}.5000 cycles later, the device's capacitance remained constant. After 5000 cycles, there was only a negligible loss of about 13.6 percent.[58] An aqueous electrolyte's operating potential was increased to 1.6 V, allowing for use in more industries. The $NiCo_2S_4$@rGO/N-rGO asymmetric supercapacitors worked admirably, delivering 34.1 W h kg^{-1} of energy density and 411 W kg^{-1} of power density.

Meng *et al.* synthesized 3D CoS/graphene composite (CGH) hydrogel through the hydrothermal method. As shown in Fig. 3a, a 3D gel-like 3D CoS/graphene composite is formed at various weight ratios (r) of GO and $Co(CH_3COO)_2 \cdot 4H_2O$. Fig. 3b shows the flower-like structure of CoS uniformly dispersed over graphene sheets. The unique 3D structure of CGH improves the electrolytic transfer process of ions as well as prevents agglomeration of CoS nanoparticles, giving higher electrochemical performance. The as-prepared CGH displays superior rate capability compared to bare CoS, as well as greater stability (94.8% of the specific capacitance was retained after 2000 cycles) and a higher specific capacitance of 564 F g^{-1} at 1 A g^{-1}. As shown in Fig. 3f, the weight ratios of GO and $Co(CH_3COO)_2 \cdot 4H_2O$ significantly alter the electrochemical properties of CGH. The higher electrochemical performance of CGH as compared to bare CoS is due to synergistic effects between 3D graphene and CoS as well as the unique 3D structure of graphene which enhances ion transport rates and charge-transfer kinetics.[59] Gigot *et al.* developed a supercapacitor electrode made of rGO/RuS_2 active species and RuS_2 using a green one-pot hydrothermal synthesis technique. The crystalline flakes of rGO are decorated with the amorphous RuS_2 as Ru active species. In 1 M of NaCl solution, the composite electrode provides a specific capacitance of 238 F g^{-1} at 5 mV s^{-1}. This exhibits exceptional extended cyclic stability over 15 000 cycles without any specific capacitance loss.[60]

2.3 Graphene-metal phosphides-based nanomaterials

Metal phosphides have been thoroughly analyzed recently as pseudo-capacitive electrode materials because of their excellent electric conductivity and metalloid nature.[37] They are more favorable for high-performance supercapacitors because they allow high-power electron transport faster than their competitors. Therefore, graphene-metal sulfides-based nanomaterials have been fabricated to advance the supercapacitor's performance with high energy and power densities. Ghosh *et al.* fabricated a Cu_3P@3DG nanohybrid composite electrode by using an easy chemical vapor deposition process (CVD) for electrochemical supercapacitor application.[61] The as-prepared

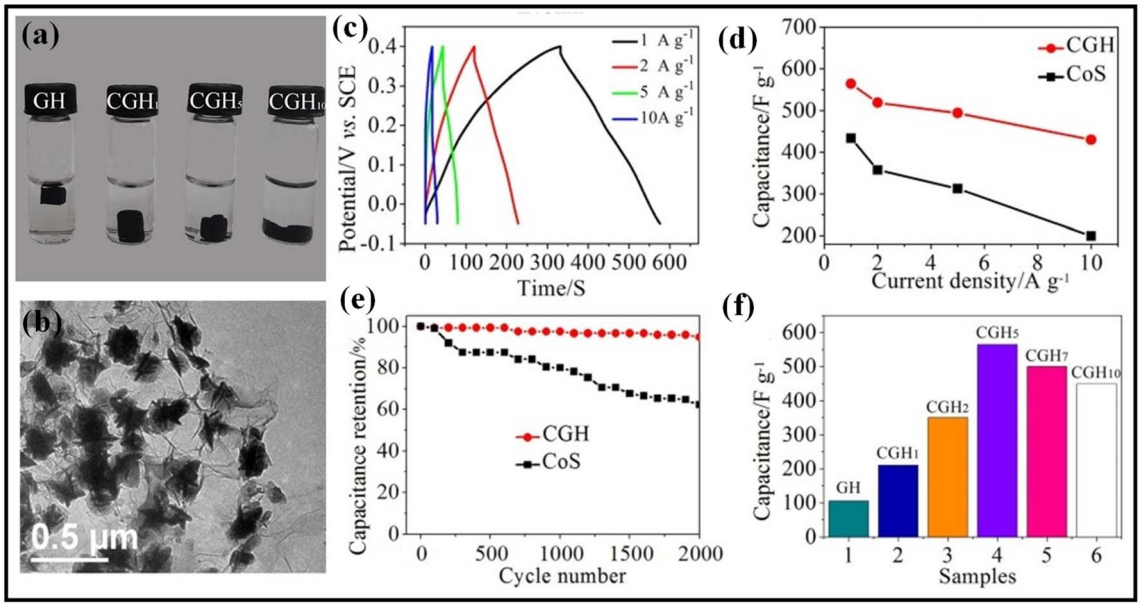

Fig. 3 (a) Images of various weight ratios of 3D CoS/graphene composite, (b) FESEM micrograph of 3D CoS/graphene composite, (c) GCD plots of 3D CoS/graphene composite at various current densities, (d) specific capacitances at various current densities, (e) the cycling stability test over 2000 cycles at 1 A g^{-1}. (f) Specific capacitances of 3D CoS/graphene composite at different weight ratios of GO and $Co(CH_3COO)_2 \cdot 4H_2O$.[59] Copyright 2016. Reproduced with permission from Springer Nature.

nanohybrid electrode (Cu_3P@3DG) demonstrated a specific capacitance value of 1095.85 F g^{-1} at a scan rate of 10 mV s^{-1} and cyclic stability of 95% after 3000 cycles at a current density of 8.97 A g^{-1}. Its capacitance is nearly 4 times higher than that of copper phosphide plates, and its stability is 1.2 times better than that of copper phosphide plates. The asymmetric device results in a superior energy density of 8.23 W h kg^{-1} and a power density of 439.6 W kg^{-1}.[61] Zheng *et al.* demonstrated a composite CoP/rGO electrode developed on Ni foam using a simple hydrothermal phosphatization process (Fig. 4a).[62] As shown in Fig. 4b and c, composites that have been prepared from (CoP/rGO) were able to carry out capacitance measurements value of 1438 F g^{-1} at a current density of 1 A g^{-1}, that is 3.43, 2.05, and 2.26 times greater than the capacitance values measured in $Co(OH)_2$/rGO, Co_3O_4/rGO, and bare.

The asymmetric device (CoP/rGO/NF//AC) has a higher energy density of 43.2 W h kg^{-1} at a current density of 1 A g^{-1} and a power density of 1010.5 W kg^{-1} and excellent long-term retention of 89 percent capacitance retention after 10 000 cycles (Fig. 4d and e). Zhang *et al.* prepared the Ni_2P–Ni@NC@G nanocomposite using the solvothermal and electrostatic self-assembly reaction process. Using highly conductive graphene in combination with NC coating that is continuously applied to the graphene surface leads to continuous electron transport channels that allow improved reaction kinetics and rate performance on the electrode.[63] The synthesized Ni_2P–

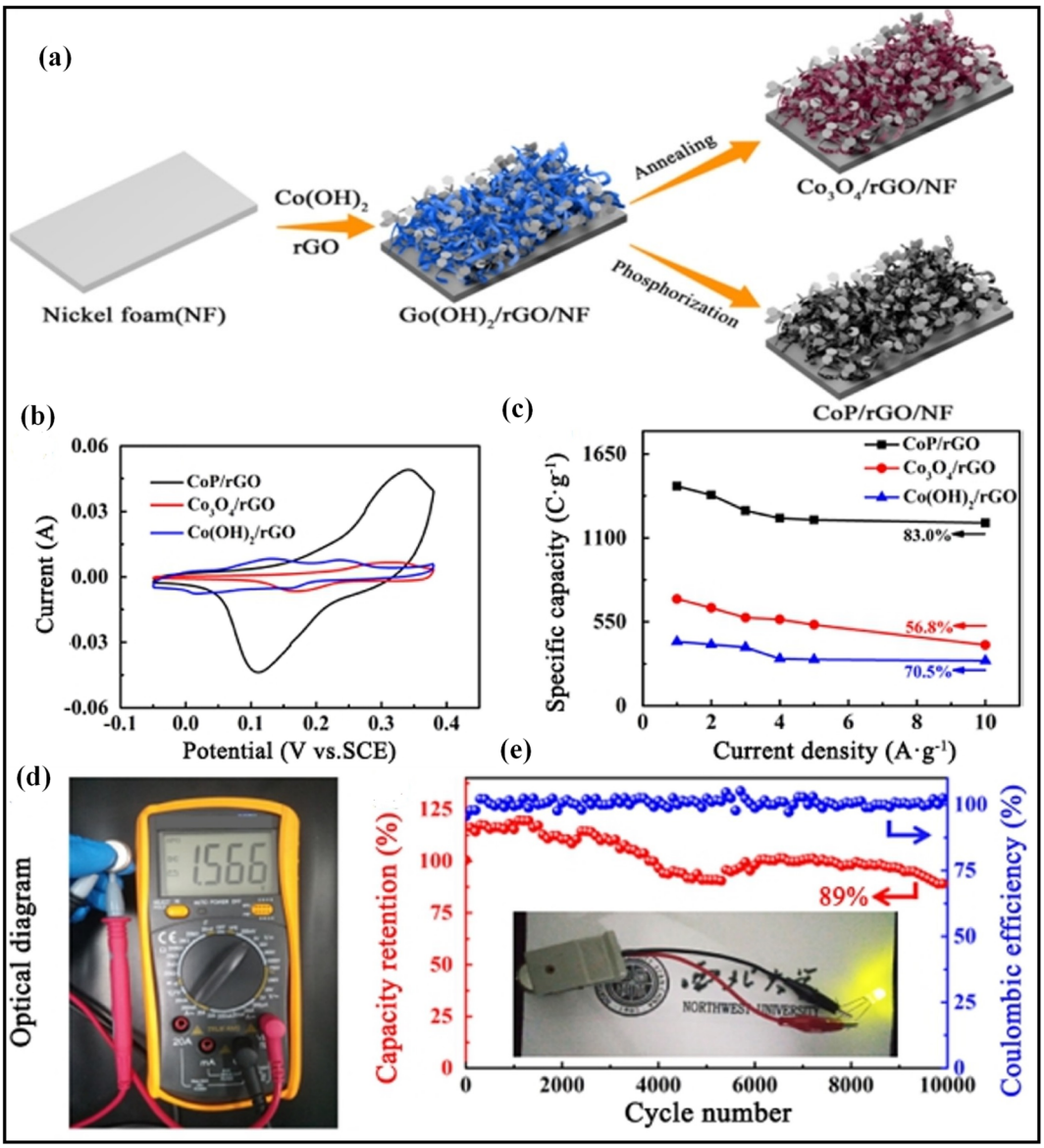

Fig. 4 (a) Schematic design of CoP/rGO electrode grown on nickel foam using a simple hydrothermal phosphatization process, (b) CV curves of CoP/rGO/NF, Co_3O_4/rGO/NF, and $Co(OH)_2$/rGO/NF electrodes at 5 mV s^{-1}, (c) comparison of specific capacities of CoP/rGO/NF, Co_3O_4/rGO/NF, and $Co(OH)_2$/rGO/NF electrodes at 1–10 A g^{-1}, (d) Digital image of the cell voltage calculated by a multimeter, (e) coulombic efficiency and Capacitance retention plots were measured for 10 000 cycles at 5 mA cm^{-2} (Inset: LED light gown by CoP/rGO/NF//AC device).[62] Copyright 2021. Reproduced with permission from the American Chemical Society.

Ni@NC@G nanocomposite material had a specific capacity of 2335 F g^{-1} at a current density of 1 A g^{-1} and outstanding long-term retention of 86.4% capacitance stability after 2000 cycles. The asymmetric device has a higher energy density of 53.125 W h kg^{-1} and a power density of 3750 W kg^{-1}. Jia *et al.* demonstrated a by chemically blowing nickel phosphide nanoparticles; they become surfaced with a thin level of carbon. Chemical blowing and phosphorylation at low temperatures generate Ni_2P nanoparticles embedded in 3-D graphene (Ni_2-P@C@rGO) Jia *et al.* demonstrate that carbon nanoparticles are coated with a layer of carbon and are obtained by blowing carbon onto the nanoparticles. They generated carbon-coated nickel phosphide nanoparticles by the chemical blowing method. Ni_2P nanoparticles were deposited by chemical blowing and then phosphorylated at low temperatures to form 3-D graphene.[64] Specific capacitances (C_s) against the current density of all as-synthesized electrode materials, Ni_2P@C@rGO-0.75 as compared to other electrode materials, has excellent capacitance performance at 1 A g^{-1} of 1338.8 F g^{-1}, and it retains 66% of its effective capacitance up to 30 A g^{-1}. ASC can produce electricity with an energy density of 34 W h kg^{-1}, and shows cycle stability of 85.2% for 10 000 cycles at a current density of 10 A g^{-1}. Mahmoud *et al.* prepared NH_4(NiCo)PO_4H_2O/GF composites using a hydrothermal technique (Fig. 5a).[65] As shown in Fig. 5b, NH_4(NiCo)$PO_4 \cdot H_2O$/GF composite shows outstanding cyclic retention as compared to pristine NH_4(NiCo)$PO_4 \cdot H_2O$ in the range of current density of 0.5 A g^{-1} and 15 A g^{-1}, due to synergic effect between GF

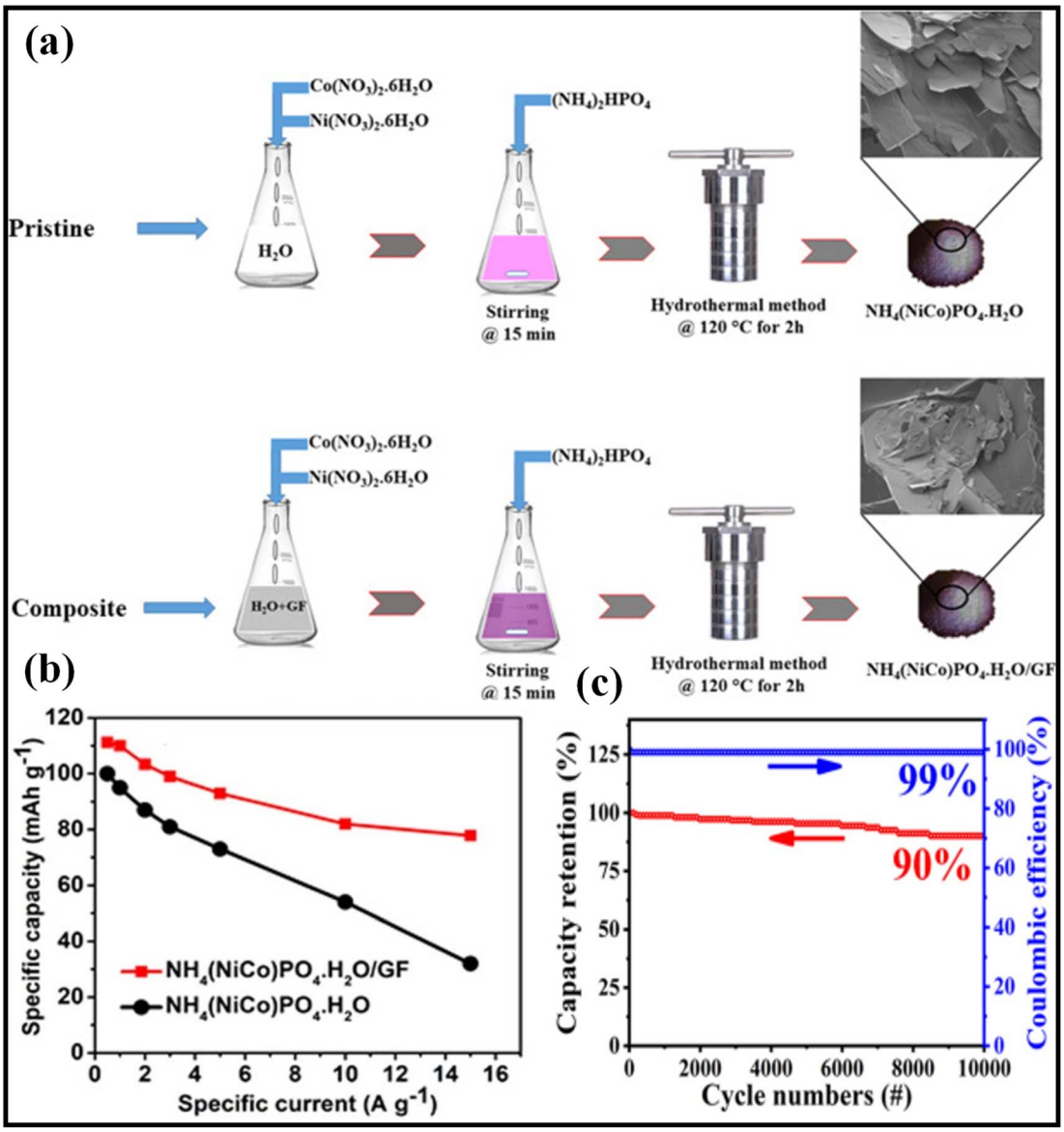

Fig. 5 (a) Schematic representation of the synthesis of NH_4(NiCo)$PO_4 \cdot H_2O$/GF composites and NH_4(NiCo)$PO_4 \cdot H_2O$, (b) specific capacity of NH_4(NiCo)$PO_4 \cdot H_2O$/GF composites and NH_4(NiCo)$PO_4 \cdot H_2O$ at a current density of 0.5–15 A g^{-1}.[65] Copyright 2021. Reproduced with permission from Elsevier. (c) Cycling stability and coulombic efficiency of NCP@P-rGO//AC at 10 A g^{-1}.[66] Copyright 2022. Reproduced with permission from Elsevier.

pristine and $NH_4(NiCo)PO_4 \cdot H_2O$. These composites were assembled in a hybrid supercapacitor as the active positive electrode. The as-fabricated device was able to preserve around 70 percent of its initial capacity while demonstrating a Columbia efficiency of 99.8 percent at 10 A g^{-1}. Javed *et al.* have shown that rGO can be integrated with nickel-cobalt phosphide electrodes by using a hydrothermal pursued by phosphorization.[66] NCP@P-rGO is an effective electrode material for creating supercapacitors. It could be used to make electrodes with higher potential. It can store a maximum of 264.9 mA h g^{-1}. The developed SC device was able to generate an extremely high energy density of 39.7 W h kg^{-1} and a very high power density of 0.79 kW kg^{-1}.

When fully charged, it was able to deliver 18.63 W h kg^{-1} of energy at a power density of 8.82 kW kg^{-1}. As shown in Fig. 5c NCP@P-rGO//AC asymmetric hybrid supercapacitor (AHS) device exhibits 90% capacity retention and 99% coulombic efficiency after 10 000 cycles; it displays excellent cyclic retention and excellent charge retention performance. Zhang *et al.* prepared the GO@NiCoP composite electrode using an easy hydrothermal process and a phosphorization process for electrochemical supercapacitor application. NiCoP has a synergistic effect that is well-suited for the adsorption of –OH at very high concentrations or deprotonation of –OH at very high concentrations, resulting in an increased electrochemical reaction potential. GO allowed for better conductivity in several composite materials. It provides many oxygen-containing functional groups that coordinate with metal cations in a number of NiCoP systems. The specific capacitance of the as-prepared electrode (GO@NiCoP) was shown as 1225 F g^{-1} at a current density of 2 A g^{-1} and good long-term stability of 104.88 percent capacitance stability after 5000 cycles.[67] Using an easy and eco-friendly process, Chen *et al.* fabricated a composite of Nickel–Cobalt phosphide with multilayer graphene (NiCoP/MLG). The synthesized NiCoP/MLG composite electrode which exhibited a specific capacitance of 1419.6 F g^{-1} at 1 A g^{-1}. Using the symmetric electrodes system, NiCoP/MLG composite demonstrated maximum specific energy and power of 32.19 W h kg^{-1} and 741.65 W kg^{-1}, respectively.[68]

2.4 Graphene-metal carbides-based nanomaterials

Recently, metal carbide-based materials have gained much attention as electrodes for enhanced electrochemical energy storage applications because of their large surface area, flake-like morphology, attractive electrical conductivity, large energy storage capability, and chemical, thermal, and electrochemical stabilities.[38] Hence, integrating meta carbide with graphene to make graphene-metal carbide-based nanomaterials can improve the supercapacitor performance profoundly. Yousef *et al.* developed the tungsten carbide with graphene nanoflakes (WC@GNFs) composite electrodes for electrochemical supercapacitor application utilizing a simple hydrothermal technique and a microwave irradiation process.[69] At a scan rate of 1 mV s^{-1}, the specific capacitance of the previously constructed electrode (WC@GNFs) was determined to be 1009.52 F g^{-1}. Excellent long-term stability was also observed, with 106 percent capacitance retention after 2000 cycles.

At a potential of 0 mV using a 1.0 M H_2SO_4 electrolyte, frequency distributions of the nanostructured graphite were found to be within a frequency range of 10 000 to 0.01 Hz according to Nyquist plots of graphene nanoflakes and tungsten carbide embedded graphene nanoflakes.[68] Visually, it was able to construct a semicircle and a straight line in the high and low-frequency zones. The composite made of titanium carbide MXene and rGO ($Ti_3C_2T_x$/rGO) was created by Gogotsi *et al.* using an easy, straightforward technique. The width of the voltage window could be increased by mixing rGO with $Ti_3C_2T_x$. A considerable rise in the capacitance value was achieved thanks to these materials' synergistic impact. In comparison to $Ti_3C_2T_x$/rGO (95 : 5 wt%), $Ti_3C_2T_x$/rGO (90 : 10 wt%), and $Ti_3C_2T_x$/rGO (80 : 20 wt%) electrodes, the synthesized $Ti_3C_2T_x$/rGO (99 : 1 wt%) composite material had a specific capacity of 254 F g^{-1} at a scan rate of 2 mV s^{-1}.[70] Due to the materials' better conductivity, the hybrid structure of $Ti_3C_2T_x$ and rGO was chosen as an electrode for electrochemical capacitors. A simple and environmentally friendly procedure was used by Kim *et al.* to create graphene-encapsulated MXene Ti_2CT_x@polyaniline (GMP) composite electrodes (Fig. 6a).[71] rectangular form of the CV curves for MXene, MP, and GMP in Fig. 6b at a scan rate of 5 mV s^{-1} denotes a rapid surface decrease of protons interacting with MXene's terminal groups. In accordance with Fig. 6c, the composite GMP displayed a specific capacitance value of 635 F g^{-1} at a current of 1 A g^{-1} and a stability rate of 97.54% after 10 000 cycles. With a greater energy density of 42.3 W h kg^{-1}, a power density of 950 W kg^{-1}, and exceptional long-term stability of 94.25% capacitance retention after 10 000 cycles at a current density of 10 A g^{-1}, the pouch cell in the asymmetric device of GMP with graphene stood out. Two pouch-type GMP/graphene asymmetric supercapacitors (p-ASC) are linked in series to power the red LED in Fig. 6d. A vanadium carbide electrode containing reduced graphene oxide (V_8C_7/rGO) nanoparticles was demonstrated by Li *et al.* utilizing a straightforward *in situ* synthesis method. The aerial capacitance of the synthesized V_8C_7/rGO nanoparticles material was 49.5 mF cm^{-2}, which is 11 times greater than that of the rGO micro-supercapacitor. Volumetric energy and power densities of 3.4 mW h cm^{-3} and 401 mW cm^{-3}, respectively, were demonstrated by the V_8C_7/rGO composite.[72] The Fig. 6e and f V_8C_7/rGO micro-supercapacitor (MSC) exhibits exceptional flexibility and maintained electrochemical performance under various bending angles from 0 to 180°.

The red LED glow image of four MSC devices taken after charging to 3.2 V at 13 A cm^{-2} is shown in Fig. 6g. Delaminated titanium carbide and reduced graphene oxide (Ti_3C_2/rGO) were combined to create the aerogel composite, and Ghosh *et al.* developed a straightforward procedure to create it.[73] The composite Ti_3C_2/rGO electrode, as constructed, had an aerial capacitance value of 171.4 mF cm^{-2} at a current density of 1 mA cm^{-2} in H_3PO_4 electrolyte, which was 4.7 times greater than that of the typical rGO electrode, as shown in Fig. 7b. With the addition of Ti_3C_2, the charge transfer resistance of the rGO aerogel decreased to 7.5, as shown in Fig. 7c, according to the

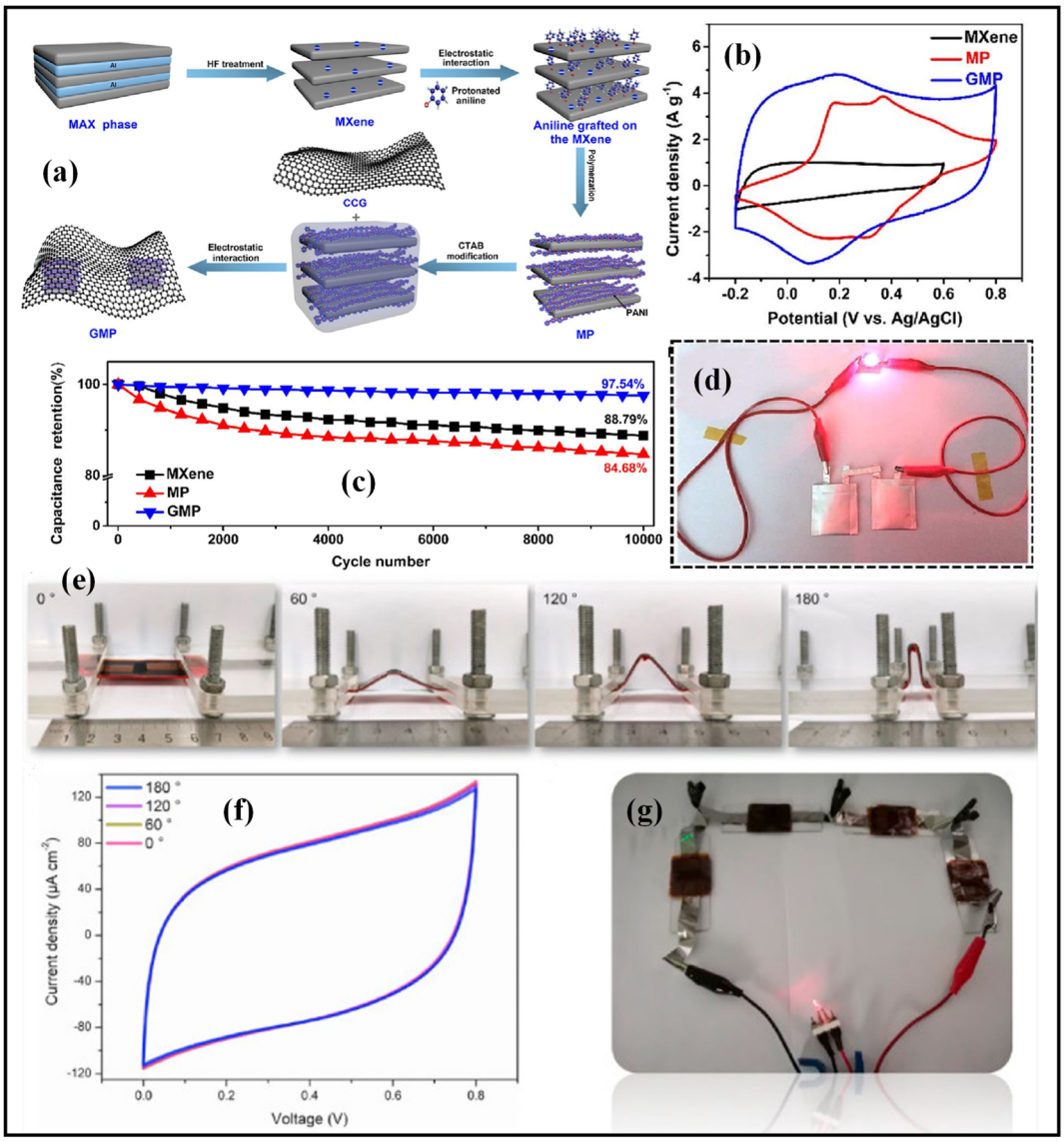

Fig. 6 (a) Scheme of preparation steps of GMP composite, (b) CV graphs of MXene, MP, GMP at 5 mV s^{-1}, (c) retention test outcomes of the MXene, MP, and GMP at 10 A g^{-1}, (d) picture of a red LED that lights up when two series of connected pouch-type GMP//graphene asymmetric supercapacitors (p-ASCs) are connected.[71] Copyright 2018. Reproduced with permission from the American Chemical Society, superior flexibility and integrability of the V_8C_7/rGO micro-supercapacitor at 390 mW (e) Pictures, (f) CV curves at 2 mV s^{-1} under various bending angles. (g) Photographs of LED powered by four micro-supercapacitors connected in series after charging 3.2 V at 13 μA cm^{-2}.[72] Copyright 2021. Reproduced with permission from Elsevier.

EIS results. The remarkable areal energy density of the supercapacitor was 2.1 W h cm^{-2}.

By CI doping of few-layered graphene walls (OMG) using a sample modifying chloritization and an annealing approach for electrochemical supercapacitor application, Zhao *et al.* created nanoflakes of molybdenum carbide, mesoporous carbon, and few-layered graphene walls (OMG). Utilising a current density of 0.5 A g^{-1} on a 1 M H_2SO_4 electrolyte, the OMG-CI electrodes generate a specific capacitance of 250 F g^{-1}. This exceeds the OMG electrode's specific capacitance. (for 179 F g^{-1} at 1 A g^{-1}), and 109% capacitance retention after 10 000 cycles,[74] both of which are good long-term retention rates. Wen *et al.* demonstrated how to deposit MXene-based composite films with various graphene contents using inkjet printing as well as how to print thermographic MXene/graphene inks.[75] A supercapacitor constructed utilising those electrodes has an exceptional energy density of 0.53 mW h cm^{-2} and a capacitance of 183.5 F cm^{-3}. The self-stacking capability of MXene can be enhanced by depositing graphene layers on top of it. The exceptional conductivity of the underlying graphene matrix is retained in composite graphene electrodes, which also feature a large interlayer spacing that significantly shortens the path that ions must travel to reach the electrode.

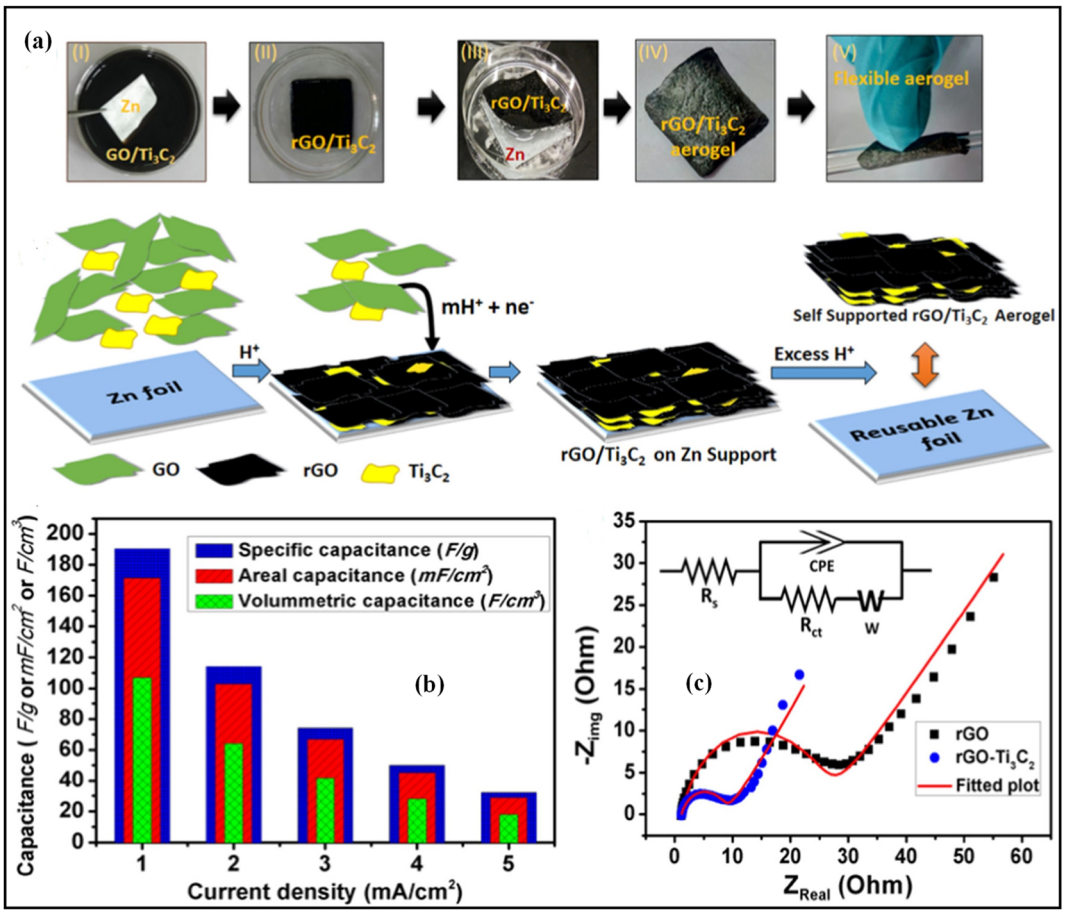

Fig. 7 (a) Different stages photographs of the fabrication process of rGO/Ti_3C_2 composite aerogel. (b) Comparison of the volumetric, gravimetric, and areal capacitance of rGO/Ti_3C_2 electrode at current density in the range of 1–5 mA cm^{-2}, (c) Nyquist plots with the fitted equivalent electrical circuit (inset) of rGO/Ti_3C_2 aerogel and rGO electrodes.[73] Copyright 2019. Reproduced with permission from Elsevier.

2.5 Graphene-metal nitride-based nanomaterials

Metal nitrides have been considered an emerging class of electrode materials because of their superior specific capacitance, good conductivity, and excellent retention.[38] As compared to the bulk, they show the better electrochemical performance improvement due to larger surface area, better activity, and high electric conductivity. Therefore, combining metal nitride with graphene to make graphene-metal nitride-based nanomaterials can significantly improve the electrochemical properties of supercapacitors. Vanadium nitride nanowires have been successfully created by Yuan *et al.*[76] utilising a straightforward freeze-casting and nitriding technique. These nanowires are coated in numerous microscopic cavities that are filled with N-doped rGO (VNNWs@rGO) composite electrodes. At a current of 0.5 A g^{-1} in a 1 M KOH electrolyte, the previously synthesised composite VNNWs@rGO-2 had a specific capacitance value of 222 F g^{-1}. The charge transfer resistance for VNNWs@rGO-2 is lower in EIS than for VNNWs@rGO-4, as demonstrated in Fig. 8b.[76] Vanadium nitride nanoparticle and graphene oxide (VNNP/GO) electrode composite was created by Ran *et al.* using an easy-to-use surface polymerization technique. An intercalation network is formed by the uniform distribution of vanadium nitride nanoparticles on graphene oxide.[77] A produced VNNP/GO composite can be capacitively improved by up to 109 F g^{-1} at a current density of 1 A g^{-1}, as shown in Fig. 8c. At a current density of 2 A g^{-1} in Fig. 8d, exceptional capacitance retention of 93% may be attained even after 5000 cycles. Although the semicircular diameter of the vanadium nitride and graphene oxide composite was bigger in the EIS, the low-frequency region slopes of these materials were lower than those of pristine vanadium nitride, indicating low diffusion resistance. For use in supercapacitors, Bendavid *et al.* created TiN nanoparticles using a straightforward, scalable, one-step transferred arc technique. On vertical graphene (VG), a plasma support material, the TiN nanoparticles are deposited to form electrodes that allow supercapacitors to be supercharged. The created electrode demonstrated remarkable long-term stability with 89.5% capacitance stability after 10 000 cycles, which is 4 times greater than that of commercial TiN deposited vertical graphene hybrid. Areal capacitance was 9.0 mF cm^{-2} at a scan rate of 100 mV s^{-1} for the manufactured electrode.[78] The supercapacitor demonstrated an exceptional 6.1 W h cm^{-2} energy density and 2718.4 W cm^{-2} power density. Mesoporous carbon nitrides with graphene aerogel (MCN/GA) composite electrode

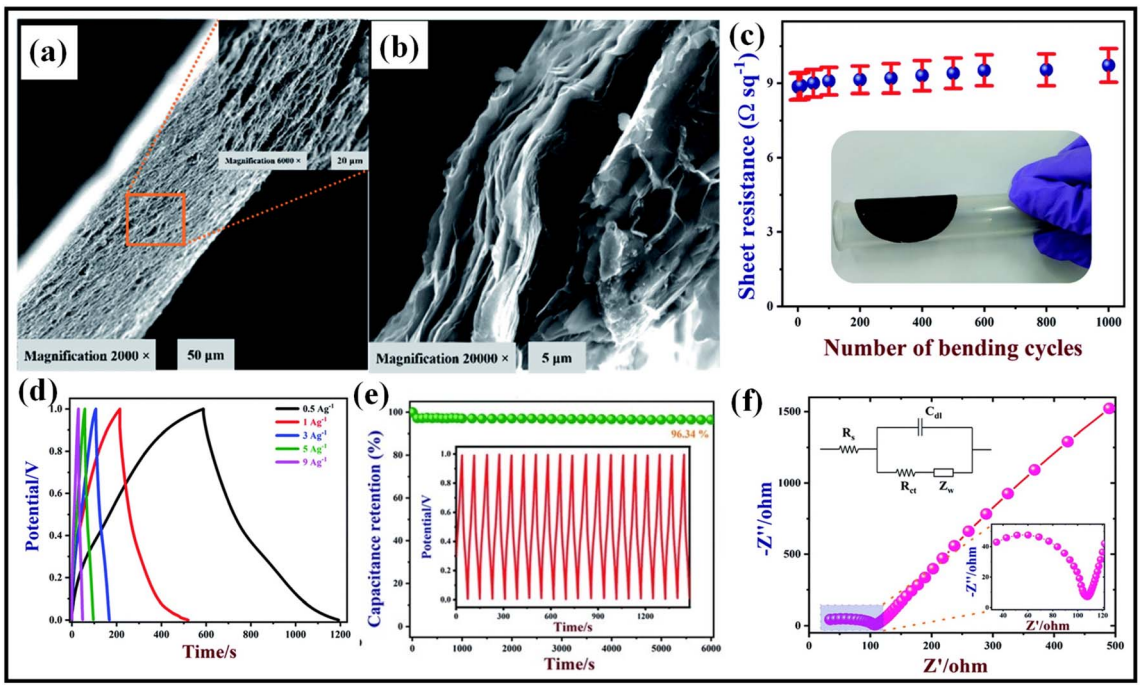

Fig. 8 (a) Low and (b) high magnification FE- SEM images of BN/GrP, (c) sheet resistance *vs.* number of bending cycles plot of BN/GrP, (d) charge–discharge plots of BN/GrP at various current densities of 0.5, 1, 3, 5, 9 A g^{-1}, (e) cyclic stability study of BN/GrP over 6000 cycles at current density of 4 A g^{-1}, (f) EIS study of BN/GrP at a frequency range of 0.1 Hz to 1000 kHz.[84] Copyright 2021. Reproduced with permission from the Royal Society of Chemistry.

was created by Zhang *et al. via* a quick nano hard-templating procedure for electrochemical supercapacitor use. At a scan rate of 3 mV s^{-1}, the constructed MCN/GA composite had a high specific capacitance of 240 F g^{-1}, which is more notable than the MCN and GA electrodes (for 142 F g^{-1} and 174 F g^{-1}). The MCN-GA symmetric device demonstrated 94 percent capacitance retention after 10 000 cycles and had an increased energy density of 11.6 W h kg^{-1} and a power density of 8.0 kW kg^{-1}.[72] A single prototype device could power a small motor (3.3 V, 30 mW) and move a rotor, demonstrating its potential use as a power source (Fig. 8e).[79] By using a straightforward one-step chemical reduction technique for electrochemical supercapacitor application, Swain *et al.* synthesised the gallium nitride with rGO (GaN/rGO) nanocomposite electrode at different gallium nitride concentrations.[80] The manufactured (GaN/rGO) electrode shown cyclic retention with capacitance stability of 75% after 950 cycles and a specific capacitance value of 454 at a scan rate of 10 mV s^{-1} in 1 M H_2SO_4. Additionally, a very low charge transfer resistance was attained, allowing for a maximum charge transfer resistance of 2.36 for the EIS research. A tungsten nitride with reduced graphene oxide fibre (WN/rGOF) nanocomposites electrode was achieved by Kim *et al.* utilising a straightforward hydrothermal technique. The as-prepared nanocomposite WN/rGOF showed a higher capacitance value of 16.29 F cm^{-3} at a current density of 0.05 A cm^{-3}, which is 7.5 times and 1.75 times bigger than the conventional rGOF and WO_3-rGOF supercapacitor. It also shows outstanding long-term retention with 84.7% cyclic stability after 10 000 cycles.[81] In order to create A-BNQD/rGO, Lee *et al.* chemically coupled reduced graphene oxide (rGO) and amine-functionalized boron nitride quantum dot (A-BNQD).[82] They found that this combination had a higher specific capacitance of 256.8 F g^{-1} than bare rGO at a current density of 1 A g^{-1}, which was caused by the intense interfacial bonding between the two materials. A-BNQD/rGO also exhibits outstanding cyclic stability with a 94.38% average over 10 000 cycles.

Further Byun *et al.* fabricated van der Waals heterostructures of boron nitride (h-BN) and graphene hybrid film through a simple solution-based method. BN/rGO hybrid film with a 0.5 : 4 weight ratio shows a higher integrated area in its CV at a fast scan rate, indicating higher rate capability, and excellent volumetric capacitance.[83] To study the flexibility of the BN/rGO hybrid film, a solid-state model device was fabricated. The solid-state BN/rGO hybrid device showed a stable volumetric capacitance of 95 F cm^{-3} at a scan rate of 50 mV s^{-1} over 1000 bending cycles. No drastic change in IR drop in the charge/discharge study and 100% retention of original capacitance after different bending angles, indicates longer stability and flexibility of the solid-state BN/rGO hybrid device. Rajendran *et al.* adopted a simple vacuum filtration technique for the fabrication of flexible hexagonal boron nitride incorporated graphene paper (BN/GrP).[84] Fig. 8a and b show the low and high magnification FE-SEM images of a cross-sectional view of BN/GrP. The thickness of BN/GrP was 21 μm and all sheets in BN/GrP are well connected and well stacked. The sheet resistance and flexibility of the BN/GrP were tested over 1000 bending cycles at 60° bending angle. As shown in Fig. 8c, the sheet resistance increased by about 8.7% over 1000 bending cycles, indicating

high mechanical stability due to the interconnected network of the film. From the GCD plot in Fig. 8d, the specific capacitance of BN/GrP is 321.95 F g^{-1} at 0.5 A g^{-1} current density. Galvanostatic charge/discharge cycles were used to test the manufactured flexible electrode's stability, and the results revealed 96.3% retention even after 6000 cycles (Fig. 8e). In an electrolyte of 0.1 M KCl and $Fe(CN)_6^{4-/3-}$, the electrochemical impedance spectroscopy (EIS) spectra of BN/GrP were recorded. As shown in Fig. 8f, The circumference of the semicircle revealed that the BN/GrP had a high R_{ct} of 72.1 Ω and a low equivalent series resistance of 34.75 Ω.

2.6 Graphene-polymer based nanomaterials

Because of their high specific capacitance, quick charge–discharge performance, and exceptional mechanical flexibility, conducting polymers like polyaniline (PANI), polypyrrole (PPy), and poly (3,4 ethylene dioxy thiophene) polystyrene sulfonate (PEDOT:PSS) are frequently used as a material for electrical supercapacitor electrodes.[38] By properly combining conducting polymer and graphene to create graphene-polymer-based nanomaterials, it is possible to achieve the highest capacitance value while maintaining flexibility and long-term cycling stability. According to Fig. 9a, Yildiz *et al.* created a novel reduced graphene oxide-Au nanoparticles@polyaniline (rGO-Au@PANI) nanocomposite utilising a straightforward, low-cost, two-step procedure.[84] The ternary nanocomposite is depicted in HR-TEM images in Fig. 9b, where rGO nanosheets are covered in extremely thin polymeric layers.[85] This work proved that it was possible to successfully manufacture Au nanoparticles with diameters ranging from 5 to 20 nm. The electrode maintained 86.9% of its initial specific capacitance over 5000 cycles at a current of 2 A g^{-1}, and its specific capacitance was shown to be 212.8 F g^{-1} at 1 A g^{-1} in 1 M H_2SO_4. Molybdenum trioxide (MoO_3) and polypyrrole (PPy) were integrated into reduced graphene oxide (rGO) in a three-step environmentally friendly process by Deng *et al.* to create MoO_3/PPy/rGO electrodes.[86]

The electrochemical performances of the MoO_3/PPy/rGO, MoO_3/PPy, MoO_3/rGO, and bare PPy were studied by CV and

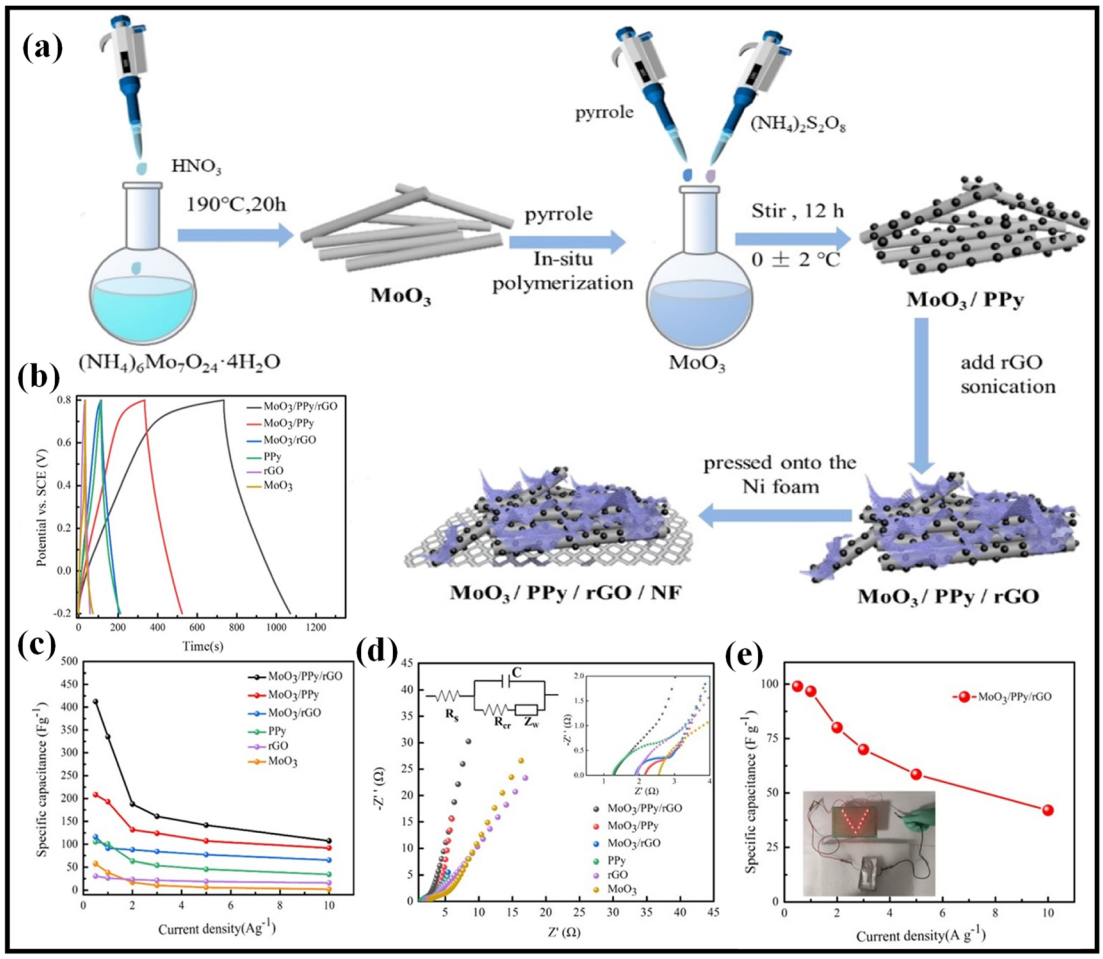

Fig. 9 (a) Schematic representation of the preparation of MoO_3/PPy/rGO composite, (b) charge/discharge plots at the current density of 1 Ag^{-1} for as-prepared electrodes, MoO_3/PPy/rGO, (c) specific capacitances of as-prepared electrodes at the current densities of 0.5 to 10 A g^{-1}, (d) Nyquist curves of as-prepared electrodes, and (e) specific capacitance of the MoO_3/PPy/rGO//MoO_3/PPy/rGO symmetric supercapacitor at various current densities (inset: photographs of LED powered by MoO_3/PPy/rGO//MoO_3/PPy/rGO symmetric supercapacitor).[86] Copyright 2021. Reproduced with permission from the American Chemical Society.

GCD tests. The GCD plots at current densities of 0.5 to 10 A g^{-1} of as-prepared electrodes were represented in Fig. 9b. In comparison to MoO_3/PPy, MoO_3/rGO, and bare PPy, the MoO_3/PPy/rGO electrode had the highest specific capacitance of 412.3 F g^{-1} at a current density of 0.5 A g^{-1}, as shown in Fig. 9c. This is due to the cooperative action of rGO sheets, PPy nanoparticles, and MoO_3. The charge transfer resistance (R_{ct}) of various as-prepared electrodes was examined by Electrochemical impedance spectroscopy (EIS) analysis (Fig. 9d). MoO_3/PPy/rGO electrodes showed R_{ct} value of 0.01, which is the lowest as compared to MoO_3 NWs (0.45), rGO (0.28), PPy, (0.29) MoO_3/rGO (0.46), which is due to high conductive nature of PPy and rGO that enhances the electron transport properties within the electrodes. In addition, a symmetric supercapacitor was fabricated using two MoO_3/PPy/rGO electrodes for practical use of MoO_3/PPy/rGO electrode material. Specific capacitance of the MoO_3/PPy/rGO//MoO_3/PPy/rGO symmetric supercapacitor at various current densities is shown in Fig. 9e.As shown in Fig. 9e, MoO_3/PPy/rGO//MoO_3/PPy/rGO symmetric supercapacitor attained highest specific capacitance of 99 F g^{-1} at a current density of 0.5 A g^{-1}. LED powered by MoO_3/PPy/rGO//MoO_3/PPy/rGO symmetric supercapacitor showed the practical application. The as-fabricated symmetric supercapacitor retained 86.2% of specific capacitance at a current density of 2 A g^{-1} over 6000 cycles. Qin *et al.* prepared a composite of reduced graphene oxide with polyaniline using a simple strategy.[87] By producing a high specific capacitance of 853.7 F g^{-1} at a current density of 1 A g^{-1}, the resulting composite material (rGO/PANI-100) outperformed rGO/PANI-30, rGO/PANI-60, rGO/PANI-150, rGO/PANI-200, and rGO/PANI-250 (741, 733, 714, 691, and 666 F g^{-1}) (Fig. 9c). With a greater energy density of 14.8 W h kg^{-1} and a lower power density of 6.7 kW kg^{-1}, the ASSSC device based on the rGO/PANI composite hydrogel sheet in Fig. 9d exhibits competitive capacitive characteristics. The as-prepared rGO/PANI-100 composite maintained 92.6% of its early capacitance up to 8000 cycles indicating its excellent cyclic stability. Chen *et al.* synthesized an rGO/PANI/PVA composite using a facile electrospinning process and fabricated it as an electrode for supercapacitor applications. When rGO concentrations was 0.2 percent, the diameters of rGO/PANI/PVA composite nanofibers were uniform and these did not stick to any of the beads or drops in the mixture. When compared to PANI/PVA electrode nanofibers (for 105 F g^{-1} at 1 A g^{-1}), the produced rGO/PANI/PVA composite displayed a higher specific capacitance of 174 F g^{-1} at 1 A g^{-1}. The slope of the rGO/PANI/PVA nanofiber curves is greatest in the low-frequency range, according to EIS measurements. This suggests that nanofibers have very low resistance and quickly conduct ions.[88]

Ghosh *et al.* developed the MnS/GO/PANI nanocomposite using a straightforward chemical oxidative polymerization method. As illustrated in Fig. 9e,[89] the MnS/GO/PANI nanocomposites demonstrated outstanding long-term cyclic stability

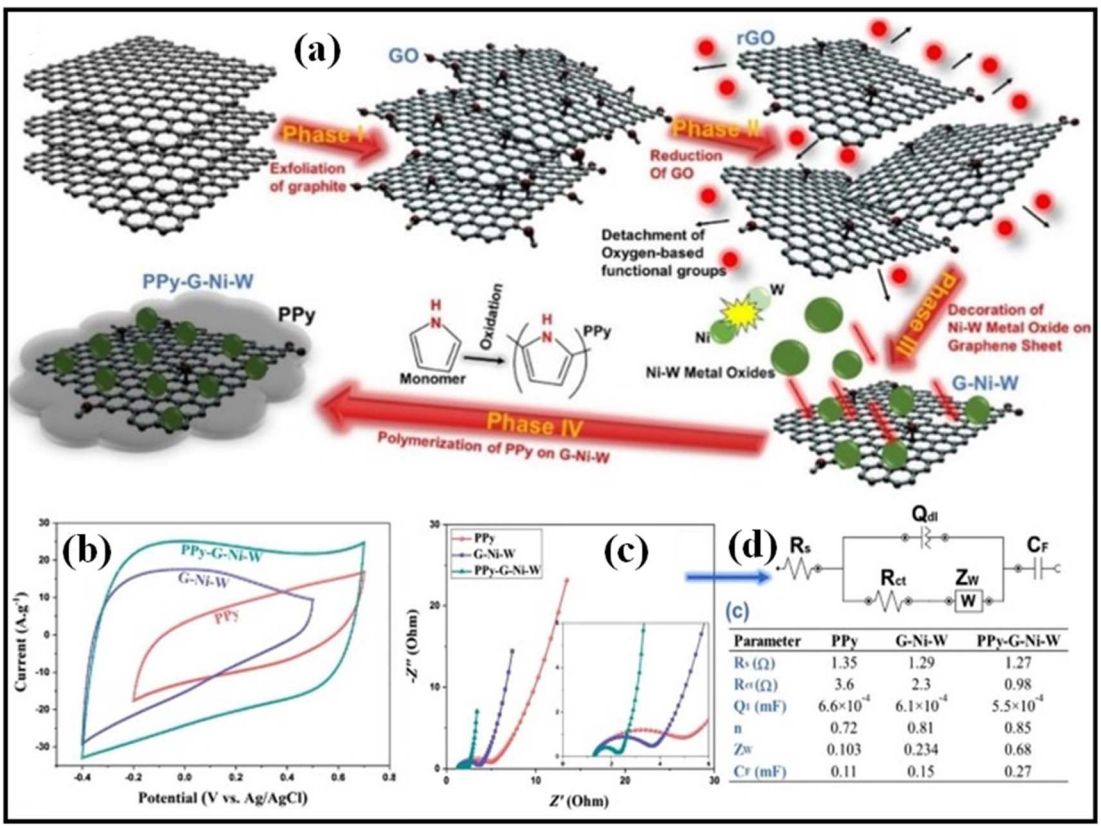

Fig. 10 (a) Schematic illustration of four-step nanomaterials processing, (b) CV curves (c) Nyquist curves with the zoomed part (inset) and its fitted circuit; (d) fitted EIS parameters of all prepared electrode materials.[92] Copyright 2021. Reproduced with permission from Elsevier.

with a capacitance stability of 95.6 percent after 1000 cycles and a specific capacitance of 822 F g^{-1} at a scan rate of 10 mV s^{-1} in 6 M KOH. In the as-prepared ternary nanocomposite MnS/GO/PANI, efficient faradaic reactions are created by improved interfacial contacts between materials and electrolytes. Zhuo *et al.* used a simple *in situ* polymerization procedure to demonstrate a composite of ZnS/rGO/PANI electrodes. For ZnS/rGO ternary composites with polymer coatings, four comparable mass ratio estimates were produced. In 3-electrode and 2-electrode systems, respectively, the produced ZnS/rGO/PANI composites showed specific capacitances of 1045.3 F g^{-1} and 722 F g^{-1} at a current density of 1 A g^{-1}. A 2-electrode device's casing has a maximum power density of 18 kW kg^{-1} and a maximum energy density of 349.7 W h kg^{-1}. In a 3-electrode and a 2-electrode system, respectively, the cyclic stability performance of ZnS/rGO/PANI composite electrodes is 160% and 76.1%.[90] For use in electrochemical supercapacitors, Kim *et al.* created a $ZnCo_2O_4$@N-GO/PANI hybrid nanocomposite electrode utilising a simple hydrothermal technique. In comparison to $ZnCo_2O_4$@N-GO, $ZnCo_2O_4$@N-GO/PANI displayed improved performance, high porosity, strong conductivity, and catalytic properties. The $ZnCo_2O_4$@N-GO/PANI nanocomposites demonstrated 720 F g^{-1} specific capacitance at 10 mV s^{-1} scan rate in 3 M KOH with exceptional long-term stability of 96.4 percent cyclic stability after 10 000 cycles. The Nyquist plot for $ZnCo_2O_4$@N-GO/PANI displays a single semicircle and a linear section, supporting the benefit of using PANI samples in supercapacitors.[91] In order to create a durable supercapacitor that could provide optimal specific capacitance, S. Alireza Hashemi *et al.* produced an electrode material by synthesizing a polymeric structure called PPy and a graphene nanosheet decorated with a hybrid metal oxide complex of tungsten and nickel (Fig. 10a).[92] PPy-G-Ni-W exhibited a significantly greater current density than G-Ni-W and naked PPy, as illustrated in Fig. 10b. The lowered R_{ct} of the PPy-G-Ni-W in comparison to G-Ni-W and bare PPy shows the optimal material for supercapacitor applications, according to the EIS results in Fig. 10c and d. rGO nanoflakes were piled on top of one another in a 2D structure created by a metal complex of nickel–tungsten (G-Ni-W), which improved the conductance and stability of rGO and reduced the detrimental effects of nickel and tungsten metal oxide complexes.

The 2D design of the structure gave it a wide surface area. The alloy G-NiW, which combines nickel and tungsten, increases the rGO nanoflakes' surface area, electron channel frequency, specific capacitance, and cyclic retention. PPy, a highly conductive polymer with electroconductive components, was also modified to give it a very steady capacitance and cycle stability. A hybrid platform with a 2D structure was found to be capable of offering a remarkable specific capacitance of 597 F g^{-1} and maintaining 98.2% of its performance after 5000 charges and discharges in this latest study. To overcome its drawbacks and improve its capacitance and cyclic retention, PPy was strengthened with G-Ni-W flakes. This may result in the

Table 2 The SC performance of recently developed various graphene-based nanomaterials as supercapacitor applications[a]

Working electrodes	Synthetic methods	Electrolyte	Specific capacitance (F g^{-1})	Current density (A g^{-1})	Cyclic stability	Ref.
MnO_2/GF	Electrodeposition	0.5 M Na_2SO_4	672	1	98%@10 000 cycles	43
Co_3O_4@rGO@CDs	Microwave	2 M KOH	936	0.5	88%@10 000 cycles	45
CeO_2/rGO	Hydrothermal	2 M KOH	301	0.5	91%@5000 cycles	46
$NiCo_2O_4$/rGO	Freeze-drying	6 M KOH	1388	0.5	90.2%@20 000 cycles	50
$MnCo_2O_4$/3DG	Hydrothermal	3 M KOH	503	1	97.4%@5000 cycles	51
Ni_3S_2/3D G/NF	CVD	6 M KOH	2585	1	88.9%@5000 cycles	56
NiS/Ni_3S_4@rGO	Hydrothermal	6 M KOH	827	5	88%@5000 cycles	57
$NiCo_2S_4$@rGO	Solvothermal	6 M KOH	2418	1	86.4%@5000 cycles	58
CoS/G	Hydrothermal	6 M KOH	564	1	94.2%@2000 cycles	59
Cu_3P@3DG	CVD	1 M Na_2SO_4	849.81	1.28	95%@3000 cycles	61
CoP/rGO	Hydrothermal	6 M KOH	3595	1	89%@10 000 cycles	62
Ni_2P–Ni@NC@G	Hydrothermal	3 M KOH	2335.5	1	86.4%@2000 cycles	63
NiCoP@GO	Hydrothermal	3 M KOH	1125	2	104.8%@5000 cycles	67
WC@GNFs	Microwave	1 M H_2SO_4	447.89	1	106%@2000 cycles	69
Ti_2CT_x@PANI/G	Self-assembly	1 M H_2SO_4	635	1	—	70
Mo_2C–Cl/G	Self-organization	6 M KOH	220	0.5	109%@10 000 cycles	74
VNNWs@rGO	Freeze-casting	1 M KOH	222	0.5	—	76
VNNP@GO	Electro-polymerization	2 M KOH	109.7	1	93%@5000 cycles	77
GaN-rGO	Chemical reduction	1 M H_2SO_4	146.1	1	75%@950 cycles	80
A-BNQD/rGO	Chemical coupling	2 M KOH	256.8	1	94.3%@10 000 cycles	82
Au@PANI-rGO	*In situ* polymerization	1 M H_2SO_4	212.8	1	86.9%@5000 cycles	85
MnS/GO/PANI	*In situ* polymerization	6 M KOH	773	1	81.6%@5000 cycles	89
ZnS/rGO/PANI	Hydrothermal	6 M KOH	1045.3	1	76.1%@1000 cycles	90
$ZnCo_2O_4$@NGO/PANi	Thermal reduction	3 M KOH	636	1.5	96.4%@10 000 cycles	91
PPy-G-Ni–W	*In situ* polymerization	1 M Na_2SO_4	557	1	98.2%@5000 cycles	92

[a] Abbreviations: GF: graphene foam, CDs: carbon dots, rGO: reduced graphene oxide, 3DG: three-dimensional graphene, NF: nickel foam, NC: nitrogen-doped-carbon, G: graphene, GO: graphene oxide, GNFs: graphene nanoflakes, A-BNQD: amine-functionalized boron nitride quantum dot, PANI: Polyaniline, VN: vanadium nitride, NW: nanowires, NP: nanoparticles.

production of very stable nanoparticle-based supercapacitors that can withstand prolonged charge–discharge cycles. Table 2 provides an overview of the SC performance of various newly produced graphene-based nanomaterials. Some of these graphene-based nanomaterials have been found to perform better than metal oxide, conducting polymers, sulphides, nitrides, and bare graphene. This is made possible by the synergistic effects of nanomaterials based on graphene as well as the customization of various mechanisms and design approaches for SC performance.

3. Conclusion and future perspective

For high-performance supercapacitor applications, we outlined recent developments in graphene-based nanomaterials with metal oxide, sulphides, phosphides, nitrides, carbides, and conducting polymers in this chapter. Due to the synergetic effects of the nanocomposite materials, such as the large surface area, higher conductance of graphene and high pseudocapacitance nature of metal oxide, sulphides, phosphides, nitrides, carbides, and conducting polymers, graphene-based nanomaterials are considered excellent electrodes for supercapacitors and outperform their bare parts in terms of specific capacitance, energy density, power density, and cyclic retention. This review also focused on the microstructural alterations in the graphene-based nanomaterials, which would be more effective for the fabrication of high-performance supercapacitors. The graphene electrode material is a superior electrode material for supercapacitor applications, but the advantages of graphene-based fabrication methods are limited because of the time-consuming processes, high production costs, and structural defects and impurities. The way graphene and based materials are prepared directly affects their properties, so it is very important to choose the right method before implementation.

With the global population continuing to urbanize and electrify, the demand for sustainable energy sources will only increase. Supercapacitors are an important piece of the puzzle in meeting this demand, as they offer several advantages over traditional batteries. However, several challenges also need to be addressed to make supercapacitors a more viable option for the future. The electrode materials utilized in supercapacitors have always been a limiting factor in the energy density that could be achieved. This has been improved in recent years by developing high-performing hybrid supercapacitors, incorporating an electrolyte composed of an ionic liquid. However, the future perspective of supercapacitors is still limited by the materials used in the electrodes. In addition, new materials are needed to improve the energy density of supercapacitors. However, there are a number of challenges linked with the usage of graphene-based nanomaterials in supercapacitor applications. One of the most significant challenges is the high cost of graphene-based nanomaterials. Another challenge is the fact that graphene-based nanomaterials are not yet commercially available in the large quantities that would be required for industrial applications. Nonetheless, the potential of graphene-based nanomaterials in supercapacitor applications is significant, and research is going on overcome the challenges associated with their use. But current methods for fabricating graphene and graphene-based hybrids are limited by complicated synthesis procedures, high production costs, and other limitations, such as structural defects and impurities. Scientists have conducted extensive research over the years. Scientists over many decades have been exploring the potential of graphene-based electrode materials for supercapacitor applications. Graphene and other graphene-based materials have advantages that outweigh their constituents' disadvantages; these advantages are enhanced by the synergistic effects of their constituent materials. It is vital to select a suitable synthesis method for producing graphene and other carbon-based hybrids before implementing them on a large scale. We have presented an overview of the research that has been done on graphene and graphene-based hybrids and also compared and contrast various fabrication methods those have been developed. Graphene has the potential to be a key component in the future of energy storage devices. Graphene-based hybrid supercapacitors, due to their unique properties, are of particular interest to researchers as they could significantly perform better on energy storage devices. Further, to better understand the relationship between material structure and electrochemical performance, several aspects should be addressed. These aspects include:

3.1 Specific surface area (SSA) and hierarchical porosity

The correlation between the specific surface area of the electrode material and its charge storage capacity is well established. A higher specific surface area results in a greater number of adsorbed ions, leading to an increased capacitance. Furthermore, a hierarchical porous structure not only enables efficient ion diffusion but also enhances the charge–discharge process.

3.2 Structural and cyclic performance

The Preservation of the structural stability of the electrode material is of utmost importance for the attainment of high-performance supercapacitors. Any structural deformation or failure leads to a decline in performance. Consequently, it is imperative to maintain the structural stability of electrode materials during multiple charging and discharging cycles. Hierarchical porous structures offer the advantages of shorter diffusion pathways and ensure contact between the electrode and electrolyte interfaces, thereby promoting improved cyclic stability.

3.3 Electrode work function

The electrode work function performs a crucial function in the surface modification of graphene for boosting charge storage. Surface modification is a fundamental and effective approach to increasing the efficiency of supercapacitors. By modifying the electrode work function, the electrochemical performance of graphene-based electrode materials can be improved considerably.

3.4 Specific capacitance and rate performance

The specific capacitance of a material depends on various factors such as surface area, pore size, synthesis methods, inherent conductivity, surface functionality, and the electrolyte utilized. A high specific capacitance is desirable, as it directly corresponds to the energy-power density. Low and high current densities and scan rates were employed to evaluate the performance of the device.

The future of graphene-based supercapacitors is promising. Researchers are working to improve their energy density and reduce costs. If these goals are achieved, supercapacitors could become the energy storage devices of choice for a broad variety of applications. Supercapacitors are becoming increasingly popular as technology improves and production costs fall. In the future, they will likely play an crucial part in electric vehicles' energy storage systems and the grid-scale energy storage systems needed to support the growth of renewable energy. The future perspective of the supercapacitor is very promising. With the ever-growing demand for renewable and clean energy. Supercapacitors will be a big part of the energy storage industry. In addition, new developments in manufacturing techniques are expected to reduce the cost of supercapacitors, making them more commercially viable. The utilization of graphene-based electrode materials in supercapacitors has generated substantial interest for energy storage applications, with evidence of superior performance across multiple domains. However, it is crucial to address a series of critical obstacles to realize their complete potential.

3.5 Energy density enhancement

Supercapacitors, while offering rapid charge and discharge capabilities, grapple with lower energy density than batteries. Elevating the energy density is crucial for broadening their application in high-energy scenarios. The unique surface adsorption and charge separation properties of supercapacitors can be optimized using graphene-based electrode materials, thus paving the way for improved energy storage.

3.6 Specific capacitance optimization

The ability of an electrode material to store charge is determined by its specific capacitance. Graphene-based electrodes, with their high specific surface areas, are promising for increasing specific capacitance. However, striking a balance between specific capacitance, electrical conductivity, and structural stability poses a challenge that demands focused attention.

3.7 Enhanced rate performance

The rapid charge and discharge capabilities of supercapacitors can be hindered by factors such as ion diffusion and electron transfer resistance. Elevating the electrochemically active surface area and implementing hierarchical porous structures in graphene-based electrode materials hold great potential for improving the rate performance of supercapacitors.

3.8 Maintaining structural stability

Preserving the structural integrity of graphene-based electrode materials is crucial for long-term optimal performance. Graphene electrodes must endure numerous charging and discharging cycles without compromising their structure, as any deviation can lead to performance decline, deformation, and eventual failure.

3.9 Cost-effective production and scalability

While graphene-based materials show promise, their large-scale production can be cost-prohibitive. Developing cost-effective synthesis methods and scalable production processes are essential for the widespread adoption of graphene-based electrode materials in supercapacitors.

3.10 Efficient synthesis and fabrication techniques

The techniques employed in the synthesis and fabrication of graphene-based electrode materials significantly influence their properties and performances. It is vital to devise efficient and scalable methods for producing high-quality graphene materials with precisely controlled structures and properties.

3.11 Mitigating the restacking of graphene particles

During fabrication, the restacking of graphene particles is a common issue, leading to reduced specific surface area and ion conductivity. Researchers have developed various methods to address this challenge, including surface modification with functional groups and the creation of graphene-based composite materials.

By systematically addressing these challenges, the advancement of high-performance supercapacitors utilizing graphene-based electrode materials will be accelerated, fostering their broader integration into energy storage systems.

Conflicts of interest

There are no conflicts to declare.

Acknowledgements

The following work is supported by the Siksha 'O' Anusandhan (Deemed to be University).

References

1 X. Mu, J. Du, Y. Zhang, Z. Liang, H. Wang, B. Huang, J. Zhou, X. Pan, Z. Zhang and E. Xie, *ACS Appl. Mater. Interfaces*, 2017, **9**, 35775–35784.
2 X. Han, K. Tao, D. Wang and L. Han, *Nanoscale*, 2018, **10**, 2735–2741.
3 J. Zhang and X. S. Zhao, *ChemSusChem*, 2012, **5**, 818–841.
4 P. Simon and Y. Gogotsi, *Nat. Mater.*, 2008, **7**, 845–854.
5 C.-A. Tseng, P. K. Sahoo, C.-P. Lee, Y.-T. Lin, J.-H. Xu and Y.-T. Chen, *ACS Appl. Mater. Interfaces*, 2020, **12**, 40426–40432.

6 R. Lakra, R. Kumar, P. K. Sahoo, D. Thatoi and A. Soam, *Inorg. Chem. Commun.*, 2021, **133**, 108929.
7 Y. Zhang, H. Feng, X. Wu, L. Wang, A. Zhang, T. Xia, H. Dong, X. Li and L. Zhang, *Int. J. Hydrogen Energy*, 2009, **34**, 4889–4899.
8 N. Kocyigit, M. Gencten, M. Sahin and Y. Sahin, *Int. J. Energy Res.*, 2020, **44**, 411–424.
9 C. Young, J. Kim, Y. V. Kaneti and Y. Yamauchi, *ACS Appl. Energy Mater.*, 2018, **1**, 2007–2015.
10 M. Mazloum-Ardakani, H. Mohammadian-Sarcheshmeh, H. Naderi, F. Farbod and F. Sabaghian, *J. Energy Storage*, 2019, **26**, 100998.
11 V. D. Nithya, *J. Energy Storage*, 2021, **44**, 103380.
12 Z. Li, J. Lin, B. Li, C. Yu, H. Wang and Q. Li, *J. Energy Storage*, 2021, **44**, 103437.
13 Y. Qin, Z. Song, L. Miao, C. Hu, Y. Chen, P. Liu, Y. Lv, L. Gan and M. Liu, *Chem. Eng. J.*, 2023, **470**, 144256.
14 Z. Song, L. Miao, Y. Lv, L. Gan and M. Liu, *Angew. Chem., Int. Ed.*, 2023, **62**, e202309446.
15 X. Shi, H. Zhang, S. Zeng, J. Wang, X. Cao, X. Liu and X. Lu, *ACS Mater. Lett.*, 2021, **3**, 1291–1299.
16 R. K. V. Prataap, R. Arunachalam, R. Pavul Raj, S. Mohan and L. Peter, *Curr. Appl. Phys.*, 2018, **18**, 1143–1148.
17 N. Kumar, S.-B. Kim, S.-Y. Lee and S.-J. Park, *Nanomater*, 2022, **12**, 3708.
18 C. He, H. Meng, X. Yao and P. K. Shen, *Int. J. Hydrogen Energy*, 2012, **37**, 8154–8160.
19 S. Prasad, G. Durai, D. Devaraj, M. S. AlSalhi, J. Theerthagiri, P. Arunachalam, M. Gurulakshmi, M. Raghavender and P. Kuppusami, *RSC Adv.*, 2018, **8**, 8828–8835.
20 P. Zhu, Z. Zhang, S. Hao, B. Zhang, P. Zhao, J. Yu, J. Cai, Y. Huang and Z. Yang, *Carbon*, 2018, **139**, 477–485.
21 M. Hassan, K. R. Reddy, E. Haque, S. N. Faisal, S. Ghasemi, A. I. Minett and V. G. Gomes, *Compos. Sci. Technol.*, 2014, **98**, 1–8.
22 B. B. Sahoo, N. Kumar, H. S. Panda, B. Panigrahy, N. K. Sahoo, A. Soam, B. S. Mahanto and P. K. Sahoo, *J. Energy Storage*, 2021, **43**, 103157.
23 L. Zhang, F. Zhang, X. Yang, G. Long, Y. Wu, T. Zhang, K. Leng, Y. Huang, Y. Ma, A. Yu and Y. Chen, *Sci. Rep.*, 2013, **3**, 1408.
24 L. Kou, Z. Liu, T. Huang, B. Zheng, Z. Tian, Z. Deng and C. Gao, *Nanoscale*, 2015, **7**, 4080–4087.
25 Z. Niu, J. Chen, H. H. Hng, J. Ma and X. Chen, *Adv. Mater.*, 2012, **24**, 4144–4150.
26 W. Chen and L. Yan, *Nanoscale*, 2011, **3**, 3132–3137.
27 Ş. Taşdemir, Z. G. Morçimen, A. A. Doğan, C. Görgün and A. Şendemir, *ACS Biomater. Sci. Eng.*, 2023, **9**, 3297–3305.
28 S. Zhang, H. Wang, J. Liu and C. Bao, *Mater. Lett.*, 2020, **261**, 127098.
29 H. Kang, Q. Ma, R. Wang, L. Zhang, S. Chen, X. Wang and C. Zhang, *Chem. Sci.*, 2022, **13**, 11883–11890.
30 L. W. Le Fevre, J. Cao, I. A. Kinloch, A. J. Forsyth and R. A. W. Dryfe, *ChemistryOpen*, 2019, **8**, 418–428.
31 P. Kamedulski, M. Skorupska, P. Binkowski, W. Arendarska, A. Ilnicka and J. P. Lukaszewicz, *Sci. Rep.*, 2021, **11**, 22054.
32 H. Fu, B. Gao, Z. Liu, W. Liu, Z. Wang, M. Wang, J. Li, Z. Feng and A. Reza Kamali, *J. Electroanal. Chem.*, 2022, **920**, 116545.
33 Y. Shen, Q. Fang and B. Chen, *Environ. Sci. Technol.*, 2015, **49**, 67–84.
34 Q. Ke and J. Wang, *J. Materiomics*, 2016, **2**, 37–54.
35 S. Yuan, X. Duan, J. Liu, Y. Ye, F. Lv, T. Liu, Q. Wang and X. Zhang, *Energy Storage Mater.*, 2021, **42**, 317–369.
36 J. Theerthagiri, R. A. Senthil, P. Nithyadharseni, S. J. Lee, G. Durai, P. Kuppusami, J. Madhavan and M. Y. Choi, *Ceram. Int.*, 2020, **46**, 14317–14345.
37 J. Theerthagiri, A. P. Murthy, S. J. Lee, K. Karuppasamy, S. R. Arumugam, Y. Yu, M. M. Hanafiah, H.-S. Kim, V. Mittal and M. Y. Choi, *Ceram. Int.*, 2021, **47**, 4404–4425.
38 J. Xiao, J. Wen, J. Zhao, X. Ma, H. Gao and X. Zhang, *Electrochim. Acta*, 2020, **337**, 135803.
39 M. Idrees, A. Mukhtar, R. Ata ur, S. M. Abbas, Q. Zhang and X. Li, *Mater. Today Commun.*, 2021, **27**, 102363.
40 Y. Huang, H. Li, Z. Wang, M. Zhu, Z. Pei, Q. Xue, Y. Huang and C. Zhi, *Nano Energy*, 2016, **22**, 422–438.
41 H. K. Hassan, N. F. Atta, M. M. Hamed, A. Galal and T. Jacob, *RSC Adv.*, 2017, **7**, 11286–11296.
42 B. S. Singu and K. R. Yoon, *J. Alloys Compd.*, 2019, **770**, 1189–1199.
43 V. Gupta, A. M. Kannan and S. Kumar, *J. Energy Storage*, 2020, **30**, 101575.
44 A. Moyseowicz, A. Śliwak, E. Miniach and G. Gryglewicz, *Compos. B. Eng.*, 2017, **109**, 23–29.
45 S. Yetiman, H. Peçenek, F. K. Dokan, M. S. Onses, E. Yılmaz and E. Sahmetlioglu, *J. Energy Storage*, 2022, **49**, 104103.
46 P. Salarizadeh, M. B. Askari, H. Beydaghi, M. Rastgoo-Deylami and S. M. Rozati, *J. Phys. Chem. Solids*, 2021, **159**, 110284.
47 Q. X. Low and G. W. Ho, *Nano Energy*, 2014, **5**, 28–35.
48 R. Kumar, S. Sahoo, W. K. Tan, G. Kawamura, A. Matsuda and K. K. Kar, *J. Energy Storage*, 2021, **40**, 102724.
49 A. Numan, N. Duraisamy, F. Saiha Omar, Y. K. Mahipal, K. Ramesh and S. Ramesh, *RSC Adv.*, 2016, **6**, 34894–34902.
50 Q. Li, C. Lu, C. Chen, L. Xie, Y. Liu, Y. Li, Q. Kong and H. Wang, *Energy Storage Mater.*, 2017, **8**, 59–67.
51 H. Wang, C. Shen, J. Liu, W. Zhang and S. Yao, *J. Alloys Compd.*, 2019, **792**, 122–129.
52 W. H. Low, S. S. Lim, C. W. Siong, C. H. Chia and P. S. Khiew, *Ceram. Int.*, 2021, **47**, 9560–9568.
53 M. F. Iqbal, A. K. M. Yousef, A. Hassan, S. Hussain, M. N. Ashiq, H. Mahmood Ul and A. Razaq, *J. Energy Storage*, 2021, **33**, 102091.
54 R. Balu and A. Dakshanamoorthy, *Inorg. Chem. Commun.*, 2022, **136**, 109148.
55 D. B. Malavekar, V. C. Lokhande, V. J. Mane, S. B. Kale, R. N. Bulakhe, U. M. Patil, I. In and C. D. Lokhande, *J. Solid State Electrochem.*, 2020, **24**, 2963–2974.
56 R. Li, W. Zhang, M. Zhang, Z. Peng, Y. Wang, Y. Liu, Y. Zheng, X. Guo, Y. Zhang, Z. Wang and T. Zhang, *Mater. Chem. Phys.*, 2021, **257**, 123769.
57 S. Nandhini and G. Muralidharan, *Electrochim. Acta*, 2021, **365**, 137367.

58 Y. Zhao, H. Zhang, Y. Lin, J. Chen, K. Li and A. Cheng, *Diamond Relat. Mater.*, 2020, **108**, 107925.
59 X. Meng, J. Deng, J. Zhu, H. Bi, E. Kan and X. Wang, *Sci. Rep.*, 2016, **6**, 21717.
60 A. Gigot, M. Fontana, C. F. Pirri and P. Rivolo, *Mater*, 2018, **11**, 57.
61 S. Kumar, S. K. T. Aziz, S. Kumar, S. Riyajuddin, G. Yaniv, L. Meshi, G. D. Nessim and K. Ghosh, *Front. Mater. Sci.*, 2020, **7**, 30.
62 H. Xing, W. He, Y. Liu, G. Long, Y. Sun, J. Feng, W. Feng, Y. Zhou, Y. Zong, X. Li, X. Zhu and X. Zheng, *ACS Appl. Mater. Interfaces*, 2021, **13**, 26373–26383.
63 Y. Zhang, L. Sun, L. Bai, H. Si, Y. Zhang and Y. Zhang, *Nano Res.*, 2019, **12**, 607–618.
64 Y. Jia, D. Hu, X. Wang, H. Zhang and P. Du, *J. Energy Storage*, 2022, **50**, 104713.
65 B. A. Mahmoud, A. A. Mirghni, K. O. Oyedotun, O. Fasakin and N. Manyala, *J. Alloys Compd.*, 2021, **883**, 160897.
66 U. Javed, G. Dhakal, A. M. Rabie, S. Iqbal, Y. R. Lee, J. Lee and J. J. Shim, *Mater. Today Nano*, 2022, **18**, 100195.
67 C. Jing, X. Song, K. Li, Y. Zhang, X. Liu, B. Dong, F. Dong, S. Zhao, H. Yao and Y. Zhang, *J. Mater. Chem. A*, 2020, **8**, 1697–1708.
68 M. Shuai, J. Lin, W. Wu, H. Kuang, W. Zhang, Q. Ling, H. Chen and S. Komarneni, *New J. Chem.*, 2020, **44**, 8796–8804.
69 D. M. El-Gendy, R. M. Abdel Hameed, A. M. Al-Enizi, M. Bakrey, M. Ubaidullah and A. Yousef, *Ceram. Int.*, 2020, **46**, 27437–27445.
70 A. M. Navarro-Suárez, K. Maleski, T. Makaryan, J. Yan, B. Anasori and Y. Gogotsi, *Batteries Supercaps*, 2018, **1**, 33–38.
71 J. Fu, J. Yun, S. Wu, L. Li, L. Yu and K. H. Kim, *ACS Appl. Mater. Interfaces*, 2018, **10**, 34212–34221.
72 H. Li, P. Tang, H. Shen, T. Hu, J. Chen, K. Chen, F. Qi, H. Yang, L. Wen and F. Li, *Carbon*, 2021, **183**, 840–849.
73 N. Radha, A. Kanakaraj, H. M. Manohar, M. R. Nidhi, D. Mondal, S. K. Nataraj and D. Ghosh, *Appl. Surf. Sci.*, 2019, **481**, 892–899.
74 Z. Kou, B. Guo, Y. Zhao, S. Huang, T. Meng, J. Zhang, W. Li, I. S. Amiinu, Z. Pu, M. Wang, M. Jiang, X. Liu, Y. Tang and S. Mu, *ACS Appl. Mater. Interfaces*, 2017, **9**, 3702–3712.
75 D. Wen, G. Ying, L. Liu, Y. Li, C. Sun, C. Hu, Y. Zhao, Z. Ji, J. Zhang and X. Wang, *J. Alloys Compd.*, 2022, **900**, 163436.
76 D. Zhao, X. Yuan, R. Wang, Q. Zhao and S. Guo, *J. Mater. Sci.: Mater. Electron.*, 2021, **32**, 21197–21205.
77 T. He, Z. Wang, X. Li, Y. Tan, Y. Liu, L. Kong, L. Kang, C. Chen and F. Ran, *J. Alloys Compd.*, 2019, **781**, 1054–1058.
78 H. Qi, S. Yick, O. Francis, A. Murdock, T. van der Laan, K. Ostrikov, Z. Bo, Z. Han and A. Bendavid, *Energy Storage Mater.*, 2020, **26**, 138–146.
79 M. Nazari, M. S. Rahmanifar, A. Noori, W. Li, C. Zhang and M. F. Mousavi, *J. Power Sources*, 2021, **494**, 229741.
80 S. Nongthombam, N. A. Devi, S. Sinha, R. Bhujel, S. Rai, W. Ishwarchand, S. Laha and B. P. Swain, *J. Phys. Chem. Solids*, 2020, **141**, 109406.
81 A. Salman, S. Padmajan Sasikala, I. H. Kim, J. T. Kim, G. S. Lee, J. G. Kim and S. O. Kim, *Nanoscale*, 2020, **12**, 20239–20249.
82 J. W. Lee, T. Kshetri, K. R. Park, N. H. Kim, O.-K. Park and J. H. Lee, *Compos. B. Eng.*, 2021, **222**, 109089.
83 S. Byun, J. H. Kim, S. H. Song, M. Lee, J.-J. Park, G. Lee, S. H. Hong and D. Lee, *Chem. Mater.*, 2016, **28**, 7750–7756.
84 J. Rajendran, A. N. Reshetilov and A. K. Sundramoorthy, *RSC Adv.*, 2021, **11**, 3445–3451.
85 Z. Çıplak, A. Yıldız and N. Yıldız, *J. Energy Storage*, 2020, **32**, 101846.
86 H. Deng, J. Huang, Z. Hu, X. Chen, D. Huang and T. Jin, *ACS Omega*, 2021, **6**, 9426–9432.
87 Z. Liu, Z. Zhao, A. Xu, W. Li and Y. Qin, *J. Alloys Compd.*, 2021, **875**, 159931.
88 Z. Chen, Y. Jiang, B. Xin, S. Jiang, Y. Liu and L. Lin, *J. Mater. Sci.: Mater. Electron.*, 2020, **31**, 5958–5965.
89 K. Y. Yasoda, S. Kumar, M. S. Kumar, K. Ghosh and S. K. Batabyal, *Mater. Today Chem.*, 2021, **19**, 100394.
90 Z. Xu, Z. Zhang, H. Yin, S. Hou, H. Lin, J. Zhou and S. Zhuo, *RSC Adv.*, 2020, **10**, 3122–3129.
91 A. Kathalingam, S. Ramesh, H. M. Yadav, J.-H. Choi, H. S. Kim and H.-S. Kim, *J. Alloys Compd.*, 2020, **830**, 154734.
92 S. Alireza Hashemi, S. Mojtaba Mousavi, H. Reza Naderi, S. Bahrani, M. Arjmand, A. Hagfeldt, W.-H. Chiang and S. Ramakrishna, *Chem. Eng. J.*, 2021, **418**, 129396.